Studies on MHC class I-mediated entry of equine herpesvirus-1 into cells

MHC class I を介したウマヘルペスウイルス 1 型の
細胞内侵入機構の解析

Michihito Sasaki

Department of Molecular Pathobiology,
Research Center for Zoonosis Control,
Hokkaido University

Contents

List of abbreviations

3T3-A68	NIH3T3-derived cell line expressing equine MHC class I A68
aa	Amino acids
APC	Allophycocyanin
β2m	β2-microglobulin
BSA	Bovine serum albumin
CHO	Chinese hamster ovary
CNS	Central nervous system
CPE	Cytopathic effects
CSPD	Disodium 3-(4-methoxyspiro{1,2-dioxetane-3, 2'-(5'-chloro)tricyclo[3.3.1.1^{3,7}]decan}-4-yl) phenyl phosphate
DIG	Digoxigenin
DMEM	Dulbecco's modified Eagle medium
DRG	Dorsal root ganglia
EBMEC	Equine brain microvascular endothelial cell
EBMECs	Equine brain microvascular endothelial cells
E. Derm	Equine dermis
EDTA	Ethylenediaminetetraaceticacid
EHV-1	Equine herpesvirus-1
FBS	Fetal bovine serum
gB	Glycoprotein B
gC	Glycoprotein C
gD	Glycoprotein D
gK	Glycoprotein K
GFP	Green fluorescent protein
HA	Hemagglutinin
HSV-1	Herpes simplex virus type 1
HSV-2	Herpes simplex virus type 2
Ig	Immunoglobulin
IRES2	Internal ribosome entry site 2
MAS	Matsunami Adhesive Silane
MEM	Minimum essential medium
MHC	Major histocompatibility complex

MOI	Multiplicity of infection
mRFP1	Monomeric red fluorescent protein 1
ORF	Open reading frame
PB	Phosphate buffer
PBMC	Peripheral blood mononuclear cells
PBS	Phosphate buffered saline
PE	Phycoerythrin
PFA	Paraformaldehyde
p.i.	post infection
PRV	Pseudorabies virus
RT-PCR	Reverse transcriptase-PCR
SDS	Sodium dodecyl sulfate
shRNA	Short hairpin RNA
SIN	Self-inactivating
VSV-G	Vesicular stomatitis virus G
VZV	Varicella-zoster virus

General Introduction

Equine herpesvirus 1 (EHV-1) is an endemic virus that affects horse populations worldwide, causing respiratory disease, abortion and a serious neurologic disease known as encephalomyelitis. Outbreaks of EHV-1 encephalomyelitis can have a severe economic impact on farms, racetracks and veterinary hospitals, and currently available vaccines are not effective to protect against EHV-1 encephalomyelitis. Histological analyses of affected horses indicate that viral infection of vascular endothelial cells leads to damage of the central nervous system due to the resulting shortage of blood supply. Although infection of these cells is closely associated with the development of encephalomyelitis, the molecular mechanisms underlying this association remain poorly understood.

Alphaherpesviruses enter target cells through sequential multistep processes. Following the initial attachment of the viruses to the cell surface, binding of viral glycoproteins to cell surface receptors triggers fusion of the viral envelope with the cell membrane, resulting in the release of viral capsid (containing viral genome) into the cytoplasm.

EHV-1 attaches to cell surface using an interaction between viral glycoprotein C (gC) and cell surface heparan sulfate. Although the role of gC is important for effective infection, it does not trigger viral entry into cells. Glycoprotein D (gD) of EHV-1 is known to be essential for EHV-1 entry into cells. However, functional gD receptor that mediates EHV-1 entry into equine central nervous system (CNS) endothelial cells remains unidentified.

In chapter 1, I performed functional cloning using an equine brain microvascular endothelial cell cDNA library and identified that equine major histocompatibility complex (MHC) class I heavy chain conferred susceptibility to EHV-1 infection in

mouse NIH3T3 cells, which are resistant to EHV-1 infection. I investigated the role of equine MHC class I in EHV-1 infection and revealed that equine MHC class I acts as an entry receptor for EHV-1 through its binding to EHV-1 gD. I further investigated the role of MHC class I in EHV-1 entry into different types of equine cells.

In chapter 2, I constructed equine MHC class I heavy chain specific-RNA probe and performed Northern hybridization to examine the level of equine MHC class I gene expression in the major organs of the adult horse body. The localization of equine MHC class I mRNA in brain tissue was investigated by *in situ* hybridization.

In this thesis, I demonstrated equine MHC class I is a bona fide receptor of EHV-1 entry into equine cells. This study provides new insights into the mechanism of EHV-1 entry into host cells and a potential way to treat and prevent this infectious disease.

Chapter 1

Equine Major Histocompatibility Complex Class I Molecules Act as Entry Receptors that Bind to Equine Herpesvirus-1 Glycoprotein D

Introduction

EHV-1, an alphaherpesvirus of the family *Herpesviridae* with a worldwide distribution, can cause respiratory disease, abortion and encephalomyelitis in horses. Although encephalomyelitis is uncommon, outbreaks of neurologic EHV-1 have caused great damage to the equine industry (Stierstorfer *et al.* 2002; Studdert *et al.* 2003; Kohn *et al.* 2006; Heerkens 2009); still, neither vaccination nor effective treatments are available for this disease. Following airborne transmission, EHV-1 infects respiratory epithelial cells and mononuclear leukocytes in the local lymph nodes, resulting in leukocyte-associated viremia. The virus then infects endothelial cells of arteries and capillaries in the CNS. Previous research has shown that the inflammation following viral replication in the endothelial cells triggers encephalomyelitis secondary to vasculitis, thrombosis and ischemic damage of the CNS (Edington *et al.* 1986; Whitwell & Blunden 1992; Stierstorfer *et al.* 2002). However, the mechanisms underlying EHV-1 endotheliotropism still need to be elucidated.

Alphaherpesviruses, including Herpes simplex virus type 1 (HSV-1), Herpes simplex virus type 2 (HSV-2), Varicella-zoster virus (VZV) and Pseudorabies virus (PRV), enter target cells through a sequential multistep process. Following the initial attachment of the viruses to the cell surface, binding of viral glycoproteins to cell surface receptors triggers fusion of the viral envelope with the cell membrane, resulting in the release of viral capsid (containing viral genome) into the cytoplasm. Various

alphaherpesvirus receptors have been previously identified, including a member of the tumor necrosis factor receptor family referred to as herpesvirus entry mediator (HVEM or HveA); the members of the immunoglobulin superfamily nectin-1 (HveC), nectin-2 (HveB) and CD155 (HveD); 3-*O*-sulfated heparan sulfate; paired immunoglobulin-like type 2 receptor α; non-muscle myosin IIA; insulin-degrading enzyme and myelin-associated glycoprotein (Montgomery *et al.* 1996; Geraghty *et al.* 1998; Warner *et al.* 1998; Shukla *et al.* 1999; Li *et al.* 2006; Satoh *et al.* 2008; Arii *et al.* 2010; Suenaga *et al.* 2010). Chinese hamster ovary (CHO)-K1 cells are naturally resistant to HSV-1, HSV-2, PRV and VZV infection, but these viruses can infect CHO-K1 cells transfected with the corresponding receptor. In contrast, EHV-1 efficiently enters and replicates in CHO-K1 cells, suggesting that EHV-1 utilizes a unique entry receptor (Frampton *et al.* 2005).

EHV-1 attaches to cell surfaces using an interaction between viral gC and cell surface heparan sulfate (Osterrieder 1999). Although the role of gC is important for effective infection, it does not trigger viral entry into cells. Entry of EHV-1 occurs either by endocytosis or by direct membrane fusion with the cell surface, depending on cell types and possibly on viral strains (Osterrieder & Van de Walle 2010). EHV-1 gD is known to be essential for EHV-1 entry into rabbit kidney (RK13) and CHO-K1 cells (Frampton *et al.* 2005; Whalley *et al.* 2007). It has been shown that αV integrin mediates entry of the EHV-1 strain L11Δgp2 into both CHO-K1 cells and equine peripheral blood mononuclear cells (PBMC) through the interaction with gD, but does not facilitate EHV-1 entry into equine vascular endothelial cells (Van de Walle *et al.* 2008). The functional gD receptors that mediate EHV-1 entry into equine vascular endothelial cells remain uncertain.

Primary cultured equine brain microvascular endothelial cells (EBMECs) are an

appropriate *in vitro* model for EHV-1 endotheliotropism studies (Hasebe *et al.* 2006). In this paper, I identified an equine MHC class I heavy chain gene that rendered NIH3T3 cells susceptible to EHV-1 infection, from a cDNA library of primary cultured EBMECs. Equine MHC class I directly interacted with EHV-1 gD, a viral protein known to be important for EHV-1 entry. Interestingly, EHV-1 dependence on MHC class I for entry was observed in equine cell types, but not in CHO-K1, which is a non-equine cell line also susceptible to EHV-1 infection. Collectively, these results suggest that equine MHC class I acts as a gD receptor for EHV-1 entry into equine cell types, including CNS endothelial cells.

Materials and Methods

Cells and viruses

NIH3T3 and 293T cells were cultured in Dulbecco's modified Eagle medium (DMEM) containing 10% fetal bovine serum (FBS). Equine dermis (E. Derm) cells (CCL-57, ATCC, Manassas, VA) were cultured in DMEM supplemented with 10% FBS and 0.1 mM non-essential amino acids. RK13 cells were cultured in Eagle's minimum essential medium (MEM) containing 10% FBS. CHO-K1 cells were cultured in DMEM/F-12 containing 10% FBS. PBMC were isolated from equine blood by density gradient centrifugation over Histopaque 1077 (Sigma, St. Louis, MO) and maintained in RPMI 1640 medium supplemented with 10% FBS, 50 μM 2-mercaptoethanol and 10 μg/ml gentamicin. Primary EBMECs were isolated from a horse brain as described previously (Hasebe *et al.* 2006) and were cultured in Medium 199 (Invitrogen, Carlsbad, CA) supplemented with 10% FBS and 10 μg/ml gentamicin. All cells were maintained at 37°C in 5% CO_2. The EHV-1 mutant Ab4-GFP contains a green fluorescent protein (GFP) expression cassette between open reading frame (ORF) 62 and ORF 63 (Ibrahim

et al. 2004). Stock viruses were cultured in E. Derm cells and titrated by plaque formation assay on RK13 cells.

Plasmids

The pIRES2-DsRed-Express2 (Clontech Laboratories, Palo Alto, CA) is a bicistronic expression vector containing the internal ribosome entry site 2 (IRES2) between the multiple cloning site and the red fluorescent marker protein DsRed-Express2 coding region. The pCXSN vector was generated by removing the c-myc epitope tag from pCMV-Myc (Clontech Laboratories) and replacing the multiple cloning site with *XhoI*, *SalI* and *NotI*. The self-inactivating (SIN) lentiviral vector constructs (CSII-CMV-MCS-IRES2-Bsd and CS-RfA-CMV-mRFP1), entry vector (pENTR4-H1), packaging construct (pCAG-HIVgp) and the VSV-G- and Rev-expressing construct (pCMV-VSV-G-RSV-Rev) were kindly provided by Dr. Miyoshi (RIKEN BioResource Center, Ibaraki, Japan). To generate the immunoglobulin (Ig) fusion proteins, an pME18S expression vector containing a mouse CD150 leader segment at the N terminus and Fc segment of human immunoglobulin G1 (IgG1) at C terminus (Satoh *et al.* 2008) was kindly provided by Dr. Arase (Osaka University, Osaka, Japan). To construct the expression plasmids, cDNA fragments of equine MHC class I B118 and β2-microglobulin (β2m) and of H2K and H2D were respectively amplified from the total RNA of E. Derm cells and of C57BL/6 mice spleen by reverse transcriptase-PCR (RT-PCR). cDNA fragments of EHV-1 gD were amplified from the genome of EHV-1 Ab4-GFP virus by PCR. A68 expression vectors containing hemagglutinin (HA) epitope tag, pCXSN-A68-HA, were constructed using pCXSN-A68 as templates. PCR primers used in this study are listed in Table 1.

Table 1 List of primers used to construct vectors

Construct name	Used primer pair	
pA68-DsRed	forward	5'-CCCTCGAGACCATGTGGGTCATGGAGCCTCG-3'
	reverse	5'-TGGAATTCTTACACTTTAGGATCCGTGAGAG-3'
pB118-DsRed	forward	5'-CCCTCGAGACCATGATGCCCCCAACCTTCCTC-3'
	reverse	5'-AGGAATTCTCACACTTTCTGTGGGAGAGA-3'
pluc-DsRed	forward	5'-AACCTCGAGATGGAAGACGCCAAAAACAT-3'
	reverse	5'-AGGAATTCTTAGAGGTCTCGATCCCACTT-3'
pCXSN-A68	forward	5'-CCCTCGAGACCATGTGGGTCATGGAGCCTCG-3'
	reverse	5'-AAGCGGCCGCTTACACTTTAGGATCCGTGAGAG-3'
pCXSN-A68-HA	forward	5'-CCCTCGAGACCATGTGGGTCATGGAGCCTCG-3'
	reverse	5'-AAGCGGCCGCTTAAGCGTAATCTGGAACATCGTATGGGTACACTTTAGGATCCGTGAGAG-3'
pCXSN-equine β2m	forward	5'-CCCTCGAGACCATGGCTCGCGTCGTGGCGCT-3'
	reverse	5'-AAGCGGCCGCTCAGAGGTCTCGATCCCACTTAAC-3'
pCXSN-gD	forward	5`-CCCTCGAGACCATGTCTACCTTCAAGCTTAT-3`
	reverse	5`-AAGCGGCCGCTTACGGAAGCTGGGTATATTTAAC-3`
pME18S-A68-IgG Fc	forward	5`-CCCTCGAGGGCTCCCACTCCATGATGTA-3`
	reverse	5`-CCCTCGAGCCATCTCAGGGTGACGGGCTC-3`
pME18S-gD-IgG Fc	forward	5`-CCCTCGAGGCGGTTCGAGGACGCCAGG-3`
	reverse	5`-CCCTCGAGACCGACGCTGATGCCCACA-3`
pENTR-H1-shβ2m1	forward	5'-TCCGTTGGGTGACGTGAGTAAACCTTTTTGGAAATCTAGACCCAGCTTTCTTG-3'
	reverse	5'-CAGCACACGTTGAGTGACATGAGCAAACCGGGGATCTGTGGTCTCATACAGAAC-3'
pENTR-H1-shβ2m2	forward	5'-TCCGTTGGAACCCAGAGACATAGCTTTTTGGAAATCTAGACCCAGCTTTCTTG-3'
	reverse	5'-CAGCACACGTTGAAACCCAGAGACACAGCGGGGATCTGTGGTCTCATACAGAAC-3'
pENTR-H1-shβ2m3	forward	5'-TCCGTTGGCATCCAAGCAGACCACTTTTTGGAAATCTAGACCCAGCTTTCTTG-3'
	reverse	5'-CAGCACACGTTGACATCCAAGCAAACCACGGGGATCTGTGGTCTCATACAGAAC-3'
pENTR-H1-shβ2m4	forward	5'-TCCGTTGAAATTGAGACACATAGCTTTTTGGAAATCTAGACCCAGCTTTCTTG-3'
	reverse	5'-CAGCACACGTTGAAACTGAGACACACAGCGGGGATCTGTGGTCTCATACAGAAC-3'
pENTR-H1-shluc	forward	5'-TCCGTATTAAGACGACTCGAAATCTTTTTGGAAATCTAGACCCAGCTTTCTTG-3'
	reverse	5'-CAGCACACGTATCAAGACGACCCGAAATCGGGGATCTGTGGTCTCATACAGAAC-3'

Complementary DNA isolation

A unidirectional EBMECs cDNA library cloned into the *EcoRI-XhoI* site of the pcDNA3.1 (+) vector (Invitrogen) in *E. coli* DH10B was plated onto two-hundred 150-mm LB agar plates containing ampicillin (100 μg/ml). Colonies were pooled by scraping and frozen in glycerol. Samples of each stock were combined into groups of 20 and cultured in LB broth with 100 μg/ml ampicillin at 37°C. Plasmid DNA was prepared using a QIAprep Spin Miniprep Kit (Qiagen, Valencia, CA). NIH3T3 cells plated in 6-well plates were transfected with plasmid DNA from each pool by using Lipofectamine 2000 (Invitrogen). Cells transfected with the GFP-expressing plasmid pEGFP-N1 (Clontech Laboratories) or with pcDNA3.1 (+) were used as controls. Thirty hours after transfection, cells were infected with Ab4-GFP at a multiplicity of infection (MOI) of 5. At 24 h post infection (p.i.), I determined the susceptibility of cells to Ab4-GFP by counting the number of GFP-expressing cells under an inverted fluorescence microscope (IX70, Olympus, Tokyo, Japan). The stock that yielded the largest number of infected cells was divided into one hundred pools. This process of subdivision and screening was repeated to obtain a single clone that yielded a plasmid with the desired phenotype.

Establishment of an equine MHC class I-expressing cell line

To obtain a cell line stably expressing the equine MHC class I heavy chain gene, I used an HIV-1–based lentiviral vector pseudotyped with the vesicular stomatitis virus G glycoprotein (VSV-G) (Miyoshi *et al.* 1998). Briefly, an MHC class I heavy chain gene was cloned into the SIN lentiviral vector construct, CSII-CMV-MCS-IRES2-Bsd. A recombinant lentivirus vector was generated by transient transfection of 293T cells with the combination of the SIN-lentiviral vector construct, pCAG-HIVgp and

pCMV-VSV-G-RSV-Rev. The supernatant containing lentivirus vector was collected after incubation of the cells at 37°C for 48 h. The A68 or B118-expressing NIH3T3 cell lines (3T3-A68 and 3T3-B118) were established by infecting NIH3T3 cells with each lentiviral vector and cultured in the presence of 10 μg/ml blasticidin S HCl (Invitrogen).

Flow cytometry

Cells were detached with cell dissociation buffer (Invitrogen) and washed with phosphate buffered saline (PBS; pH 7.4) containing 2% bovine serum albumin (BSA). Cells were stained with the anti-MHC class I monoclonal antibody PT85A, H58A, B5C (VMRD, Pullman, WA) or anti-gD polyclonal antibody (generated in my laboratory) at 4°C for 30 min. Mouse IgG2a (BD Biosciences, San Jose, CA), IgG2b and rabbit IgG (Beckman Coulter, Fullerton, CA) were used as controls. Cells were stained with an Alexa Fluor 488-conjugated anti-mouse IgG antibody (Invitrogen), allophycocyanin (APC)-conjugated anti-mouse IgG or APC-conjugated anti-rabbit IgG (Beckman Coulter) at 4°C for 30 min. Flow cytometric analysis was performed using a FACS Canto system (BD Biosciences) and the data collected was analyzed using Flowjo software (Tree Star, Ashland, OR).

Generation of Ig fusion protein

The expression vectors pME18S-A68-IgG Fc and pME18S-gD-IgG Fc were constructed by subcloning the extracellular domain of gD and A68 into pME18S expression vectors. Ig fusion proteins were expressed using the FreeStyle 293 expression system (Invitrogen) as described by the manufacturer. Briefly, 293F cells were transfected with pME18S-A68-IgG Fc and pCXSN-equine β2m (for A68-Ig expression) or pME18S-gD-IgG Fc (for gD-Ig expression) using 293fectin (Invitrogen).

Secreted Ig fusion proteins were purified on HiTrap rProtein A FF column (GE Healthcare, Buckinghamshire, UK) and buffer exchanged into PBS using an Amicon Ultra-15 centrifugal filter unit with an Ultracel-10 membrane (Millipore, Bedford, MA).

Immunoprecipitation assay

293T cells were transfected with gD expression plasmid, or with HA-tagged A68 and equine β2m expression plasmids, to obtain a high expression of A68 using 293fectin. Cells were lysed in a lysis buffer [10 mM Tris-HCl (pH 7.5), 0.5% Brij 98, 150 mM NaCl] supplemented with Complete protease inhibitor cocktail (Roche, Basel, Switzerland). Lysed proteins were incubated with Dynabeads Protein A (Invitrogen) for 1 h at 4°C after coating with Ig fusion protein. Precipitated protein complexes were eluted with 0.1 M citrate buffer (pH 3.0) and fractionated by SDS-PAGE. Proteins were transferred onto Immobilon-P transfer membranes (Millipore) and detected with anti-gD polyclonal antibody, anti-HA monoclonal antibody (Sigma) or anti-human IgG antibody (Jackson Immunoresearch, West Grove, PA).

Binding assay

To detect virions attaching to the cell surface, cells were detached and incubated with Ab4-GFP at an MOI of 20. After incubation for 1 h at 4°C, unbound virus was washed out with PBS, stained with an anti-EHV-1 polyclonal antibody (a gift from Dr. Kirisawa, Rakuno Gakuen University, Hokkaido, Japan), and analyzed by flow cytometry.

To assess Ig fusion protein binding, cells were detached and incubated with 5 μg of Ig fusion protein at 4°C for 30 min. Purified human IgG (Invitrogen) was used as a control Ig protein. Binding of the Ig fusion proteins was detected by phycoerythrin

(PE)-conjugated anti-human IgG antibody (Beckman Coulter) and analyzed by flow cytometry.

ATP depletion assay

For samples depleted of cellular ATP during viral entry, cells were preincubated in ATP depletion media composed of glucose-free, FBS-free DMEM (Invitrogen) with 10 mM 2-deoxyglucose (Sigma) and 10 mM sodium azide (Sigma) for 30 min, and infected with Ab4-GFP at an MOI of 5 (RK13 and E. Derm) or 20 (3T3-A68 and CHO-K1) for 1 h in ATP depletion media. After EHV-1 infection, cells were treated with 0.1 M citrate buffer (pH 3.0) to inactivate remaining viruses on the cell surface. The media were replaced with regular culture media and cells were cultured for 12 h at 37 °C. For samples depleted of ATP after post entry, cells were infected with Ab4-GFP in FBS-free DMEM. After viral infection, cells were incubated in ATP depletion media for 1.5 h and then the media were replaced with regular culture media. At 12 h p.i., GFP-positive cells were counted by flow cytometry. Cellular ATP levels of each cell line treated or untreated with the 2-deoxyglucose and sodium azide were measured using the CellTiter-Glo luminescent cell viability assay (Promega, Madison, WI) according to the manufacturer's instructions.

Detection of immediate early, early and late EHV-1 mRNA expression

Cells were infected with Ab4-GFP at an MOI of 5. After washing cells with PBS, total RNA was extracted at 0 h p.i. (immediately after seeding the virus) and 4 h p.i. with the TRIzol reagent (Invitrogen). After the treatment with amplification-grade DNase I (Invitrogen), RT-PCR was performed with primers specific for EHV-1

immediate early (IE), early (ICP0), and late (gB, gD, gK) genes, using the method described by Hasebe *et al.* (Hasebe *et al.* 2006).

Viral growth analysis

Cells were infected with Ab4-GFP at an MOI of 5. After incubation at 37°C for 1 h to allow viral attachment, cells were washed three times with PBS and re-fed with growth media. At 1 h p.i. (immediately after the PBS wash), 8 h p.i., and 24 h p.i., the supernatants were collected. The viral titer was determined by plaque formation on RK13 cells.

Infectivity neutralization assay

For neutralization of viral gD, EHV-1 Ab4-GFP at an MOI of 5 were incubated with anti-gD polyclonal antibody or control rabbit IgG for 30 min at 37°C, and the virus-antibody mixture was added to the cells. After incubation for 2 h, extracellular virus was inactivated by the treatment with 0.1 M citrate buffer (pH 3.0). The cells were maintained in fresh growth medium for further 12 h p.i. Viral entry was assessed by counting the number of GFP-positive cells using flow cytometry.

For competition of viral gD, 3T3-A68 cells were incubated with gD-Ig fusion protein for 30 min at 37°C, followed by the infection with EHV-1 Ab4-GFP at an MOI of 5 for 2 h. Viral entry was evaluated as described above.

For examination of the effects of anti-MHC class I antibodies, cells were incubated with 50 μg/ml of antibodies for 30 min at 37°C. The cells were infected with Ab4-GFP virus at an MOI of 5 for 2 h at 37°C. Viral entry was evaluated as described above.

Lentiviral vector expressing shRNA

Lentiviruses carrying short hairpin RNA (shRNA) were generated using the method described by Katayama *et al*. (2004). I designed shRNA constructs, shβ2m1 and shβ2m2, that were specific for the equine β2m sequence (GenBank accession number: X69083), and shβ2m3 and shβ2m4 that were specific for Chinese hamster β2m sequence (GenBank accession number: X57112). I also generated shRNAs against luciferase (shluc) as a control (Ui-Tei *et al.* 2004). Briefly, the entry vectors pENTR4-H1-shRNA were constructed by inverse PCR using the pENTR4-H1 and synthetic primers (listed in Table 1). Each entry vector was incubated with the CS-RfA-CMV-mRFP1 vector in the presence of Gateway LR Clonase (Invitrogen) for plasmid recombination. The Clonase-recombinant SIN vector constructs, CS-H1-shRNA-mRFP1, were transfected into 293T cells with the Lenti-X HT packaging system (Clontech Laboratories).

β2-microglobulin knockdown

Supernatants containing each lentivirus were applied to E. Derm or CHO-K1 cells. Transduction of shRNA into cells was confirmed by monomeric red fluorescent protein 1 (mRFP1) expression. The effect of shRNA knockdown was evaluated from the decreased level of MHC class I heavy chain expression using flow cytometry. Cells expressing shRNA were infected with Ab4-GFP at an MOI of 1 for 24 h. Fluorescence signals of mRFP1 and GFP were observed under an inverted fluorescence microscope, and images were processed using DP manager software (Olympus). GFP-positive cells were counted by flow cytometry.

Statistical analysis

Statistically significant differences were determined by Student's *t*-tests. Results are

presented as arithmetic means and bars represent standard deviations.

Accession numbers

The reported nucleotide sequence data are available in the DDBJ/EMBL/GenBank databases under accession numbers AB525079 (A68) and AB525080 (B118).

Results

Complementary DNA library screening

I first examined the attachment of EHV-1 to EBMECs, which are highly susceptible to EHV-1 infection, and to murine fibroblast-derived NIH3T3 cells, which are considered resistant to EHV-1 infection. Viral attachment was detected in both EBMECs and NIH3T3 cells by flow cytometry (Fig. 1A). However, following infection of the cells with the GFP-expressing EHV-1 mutant strain (Ab4-GFP), the GFP signal was observed in EBMECs, but not in NIH3T3 (Fig. 1B). These results suggest that NIH3T3 cells are resistant to EHV-1 infection despite efficient viral attachment to the cell surface.

I next screened an equine brain microvascular endothelial cell (EBMEC) cDNA library for sequences that rendered NIH3T3 cells susceptible to EHV-1 infection. In the first round of screening, plasmids from one group of 20 bacterial stocks from the cDNA library made 6 cells in the monolayer susceptible to Ab4-GFP infection. GFP-positive cells were entirely absent in the monolayer transfected with mock plasmids. To increase the frequency of conversion, I subdivided the bacterial stock showing the highest conversion frequency into groups of 10 and then repeated plasmid DNA transfection and screening. After five rounds of division and screening, I obtained the desired plasmid clone (pcDNA201-81-13-71-68). DNA sequencing of pcDNA201-81-13-71-68

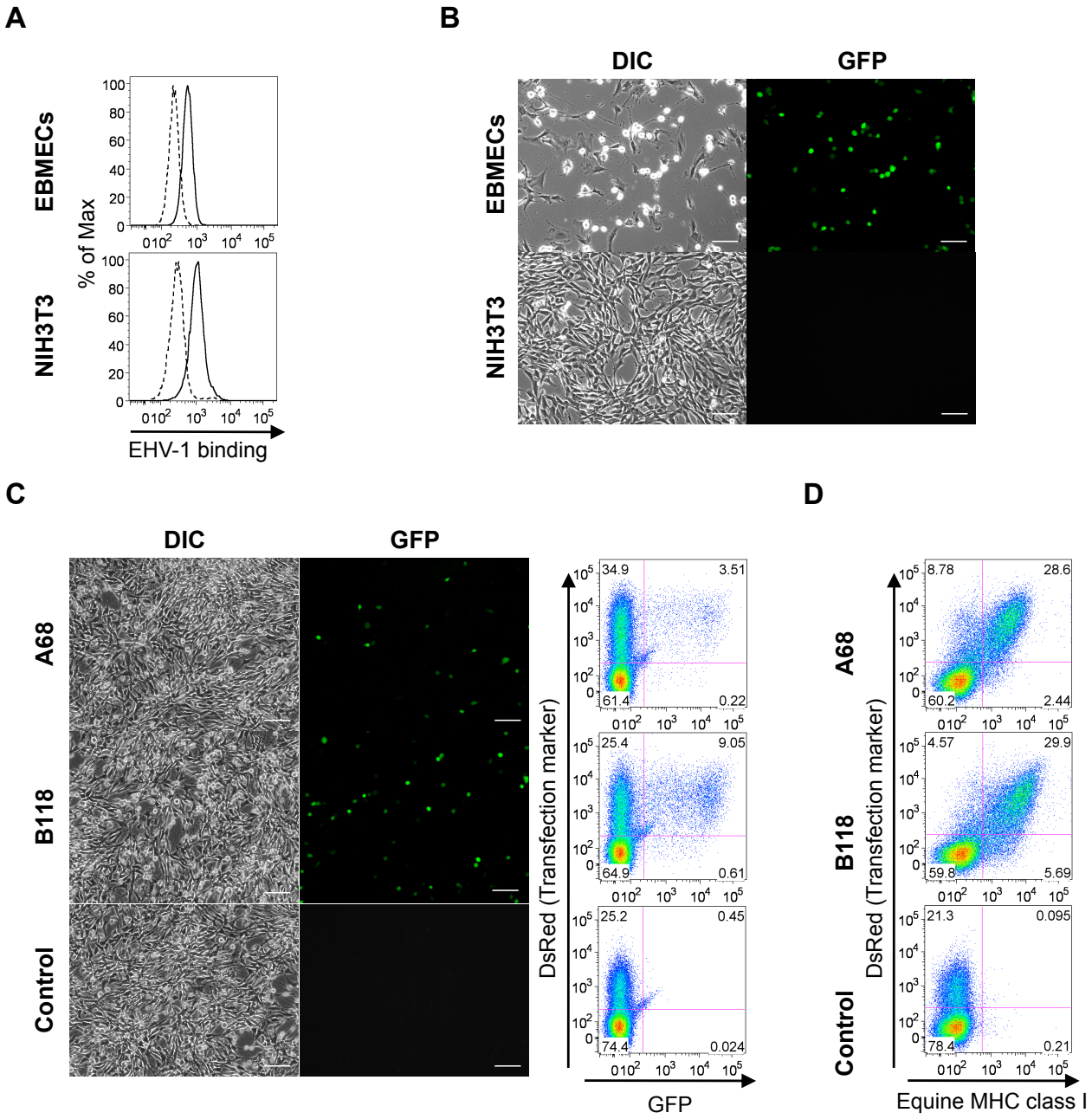

Figure 1. EHV-1 infection of NIH3T3 cells expressing equine MHC class I
(**A**) Flow cytometric detection of EHV-1 virions bound to the cell surface of EBMECs (upper panel) and NIH3T3 cells (lower panel). EHV-1–treated (solid line) and mock-treated (dashed line) cells were stained with an anti-EHV-1 antibody. (**B**) EBMECs and NIH3T3 cells were inoculated with Ab4-GFP at an MOI of 5 for 12 h. EHV-1 infected cells were identified by observing GFP signals under a fluorescence microscope. Scale bars: 100 μm. (**C**) NIH3T3 cells transiently transfected with pA68-DsRed, pB118-DsRed or pluc-DsRed were infected with EHV-1 Ab4-GFP at an MOI of 5. The number of GFP- and DsRed-positive cells was analyzed simultaneously by flow cytometry. Scale bars: 100 μm. (**D**) The expression of equine MHC class I was analyzed by flow cytometry using an anti-equine MHC class I antibody PT85A. Numbers on plots indicate the percentage of cells in the designated gate.

revealed that a cDNA insert of 1,587 base pair encoded an ORF of 365 amino acids (aa). A search of the GenBank/EMBL/DDBJ databases showed that this protein product exhibited a similarity of 91% with the equine MHC class I heavy chain *ECMHCA1* (GenBank/EMBL/DDBJ entry X71809).

According to the classification of equine MHC class I genes reported by Holmes and Ellis (Holmes & Ellis 1999), the deduced aa sequence belonged to group A of the class I sequence; therefore, I designated the cloned cDNA (GenBank/EMBL/DDBJ entry AB525079) as A68. A68 was subcloned from pcDNA201-81-13-71-68 into the expression plasmid, pIRES2-DsRed-Express2, and the resulting plasmid was designated as pA68-DsRed. After inoculation of Ab4-GFP, NIH3T3 cells transfected with pA68-DsRed displayed cytopathic effects (CPE) and GFP expression, whereas NIH3T3 cells transfected with control plasmid, pluc-DsRed encoding luciferase, showed neither CPE nor GFP expression (Fig. 1C). Nearly all GFP positive cells showed DsRed positivity by flow cytometry analysis, suggesting that EHV-1 infection occurred only in NIH3T3 cells successfully transfected with pA68-DsRed (Fig. 1C).

Because A68 was assigned to the MHC class I gene family, I evaluated whether other equine MHC class I heavy chain genes enhanced susceptibility to EHV-1 infection. A cDNA encoding equine MHC class I heavy chain that was 100% identical to the *Equine classical MHC class I allele 118 partial cds* (GenBank/EMBL/DDBJ entry AY176106) was isolated from EHV-1–susceptible equine dermal fibroblast (E. Derm) cells by RT-PCR. Because the deduced aa sequence of the isolated equine MHC class I heavy chain belonged to group B of the MHC sequence (Holmes & Ellis 1999), I designated the cloned cDNA (GenBank/EMBL/DDBJ entry AB525080) as B118 and constructed pB118-DsRed by cloning it into the pIRES2-DsRed-Express2 expression vector. NIH3T3 cells transfected with pB118-DsRed also showed CPE and GFP

expression after the inoculation with Ab4-GFP (Fig. 1C). Flow cytometry using the anti-MHC class I antibody PT85A, a monoclonal antibody that recognizes horse MHC class I but not mouse MHC class I, confirmed the cell surface expression of equine MHC class I in NIH3T3 cells transfected with pA68-DsRed or pB118-DsRed, but not in those transfected with control plasmid (Fig. 1D). I also isolated mouse MHC class I, H2K and H2D from mouse spleen cDNA and confirmed that the over-expression of murine MHC class I did not confer susceptibility to EHV-1 infection (data not shown). These results indicate that cell surface expression of equine MHC class I renders NIH3T3 cells susceptible to EHV-1 infection.

Effect of equine MHC class I expression on NIH3T3 cells

To further analyze the function of equine MHC class I molecules in EHV-1 infection, I established an NIH3T3-derived cell line that stably expresses A68 (3T3-A68). Anti-equine MHC class I monoclonal antibodies PT85A (Isotype IgG2a), H58A (Isotype IgG2a) and B5C (Isotype IgG2b) specifically reacted with A68 on the cell surface of 3T3-A68 (Fig. 2A). I attempted to neutralize viral infection by incubating cells with these anti-MHC class I antibodies. After preincubation with the antibodies or the IgG isotype controls, cells were exposed to Ab4-GFP. Viral entry was evaluated by counting the number of GFP-expressing cells using flow cytometry. PT85A treatment significantly inhibited virus entry into 3T3-A68 (inhibition of 59% as compared to the mock treatment), but H58A and B5C did not block viral entry significantly (Fig. 2B). I also investigated the neutralizing activity of anti-MHC class I antibodies on EBMECs. Expression of MHC class I on EBMECs was confirmed by flow cytometry (Fig. 2A). PT85A and H58A antibodies prevented EHV-1 entry into EBMECs (infection inhibition of 95% and 62%, respectively) (Fig. 2C). These results suggest that equine MHC class I

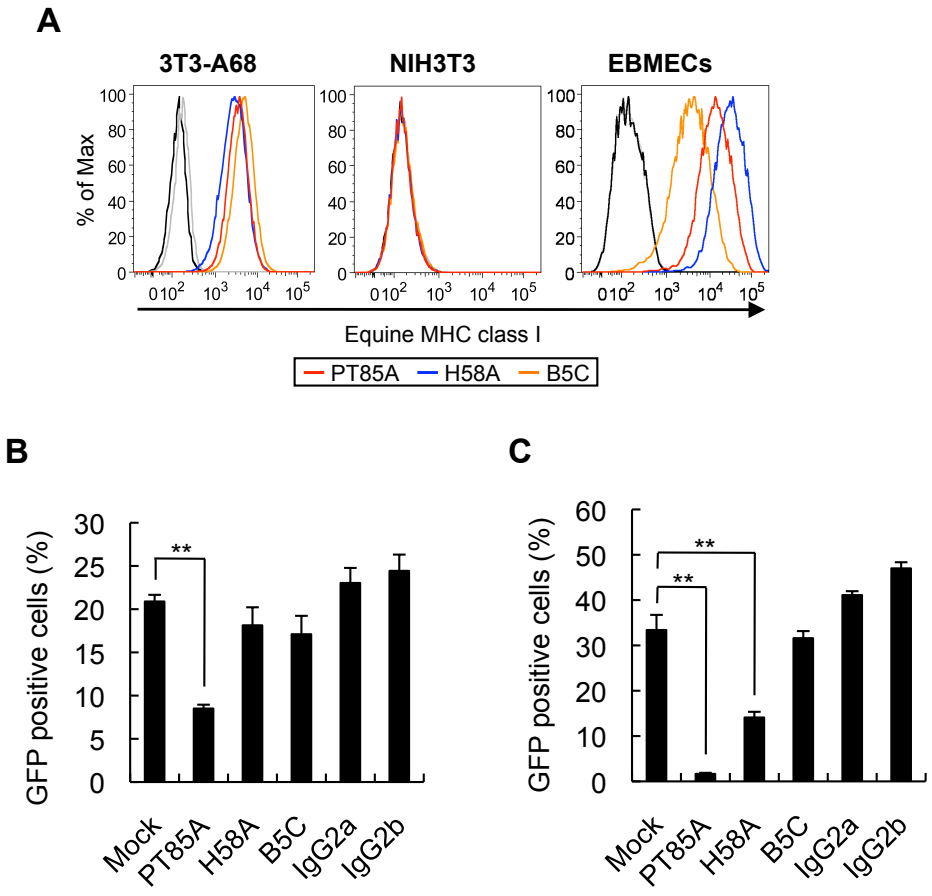

Figure 2. Inhibition of EHV-1 entry with an anti-MHC class I antibody
(**A**) Flow cytometric detection of equine MHC class I expression on 3T3-A68, NIH3T3 cells and EBMECs stained with anti-MHC class I antibody PT85A (red), H58A (blue), B5C (orange), or isotype controls IgG2a and IgG2b (black and gray, respectively). (**B** and **C**) Infectivity neutralizing assay. 3T3-A68 cells (**B**) and EBMECs (**C**) were preincubated with 50 μg/ml of anti-MHC class I or control antibodies for 30 min, and then infected with EHV-1 Ab4-GFP at an MOI of 5 in the presence of the antibody for 2 h at 37°C. After treatment with a low-pH citrate buffer to inactivate extracellular virions, incubation was continued for a further 12 h. GFP-positive cells were counted by flow cytometry. Bars represent the means from three samples and error bars show standard deviations. Statistical significance was determined by Student's *t*-tests and is indicated by asterisks (**p < 0.01).

molecules are involved in EHV-1 entry into both 3T3-A68 cells and EBMECs.

I next examined the effects of cellular ATP depletion on EHV-1 entry into 3T3-A68 cells. ATP depletion is known to inhibit endocytosis, but has no effect on herpesvirus entry by direct fusion of viral envelopes with plasma membranes (Nicola *et al.* 2003). Previous studies have suggested that entry of EHV-1 into CHO-K1 cells occurs via an endocytic mechanism (Frampton *et al.* 2007; Van de Walle *et al.* 2008), whereas entry into RK13 cells occurs by direct fusion at the cell surface (Frampton *et al.* 2007). Therefore, I used CHO-K1 and RK13 cells as positive and negative controls, respectively, for determining the effect of cellular ATP depletion on EHV-1 entry. I also used E. Derm cells as a positive control because EHV-1 entry into E. Derm cells was reduced by ATP depletion (Hasebe *et al.* 2009). An ATP depletion experiment was performed by using the method described by Hasebe *et al*. (2009) with minor modifications. To exclude the toxic influence of ATP depletion on cell viability, the effect of ATP depletion on EHV-1 entry was estimated by dividing the number of infected cells obtained from the ATP depletion media during viral infection (viral entry step) by the number of infected cells obtained from the ATP depletion media after viral infection (post viral entry step). ATP depletion during viral entry reduced EHV-1 infection in 3T3-A68 as well as CHO-K1 and E. Derm cells (Fig. 3A). In contrast, EHV-1 infection was not inhibited in RK13 cells (Fig. 3A). The observed decrease in cellular ATP levels in each cell line (Fig. 3B) suggests that EHV-1 entry into 3T3-A68 cells depends on cellular ATP, which is required for viral entry via endocytosis.

In addition, I performed RT-PCR to confirm EHV-1 gene expression in 3T3-A68 cells using specific primer sets for immediate early (IE), early (ICP0) and late (gB, gD and gK) EHV-1 genes. At 4 h p.i., all genes were detected in 3T3-A68 and E. Derm cells, whereas no viral RNA was detected in NIH3T3 cells (Fig. 4A). Because no PCR

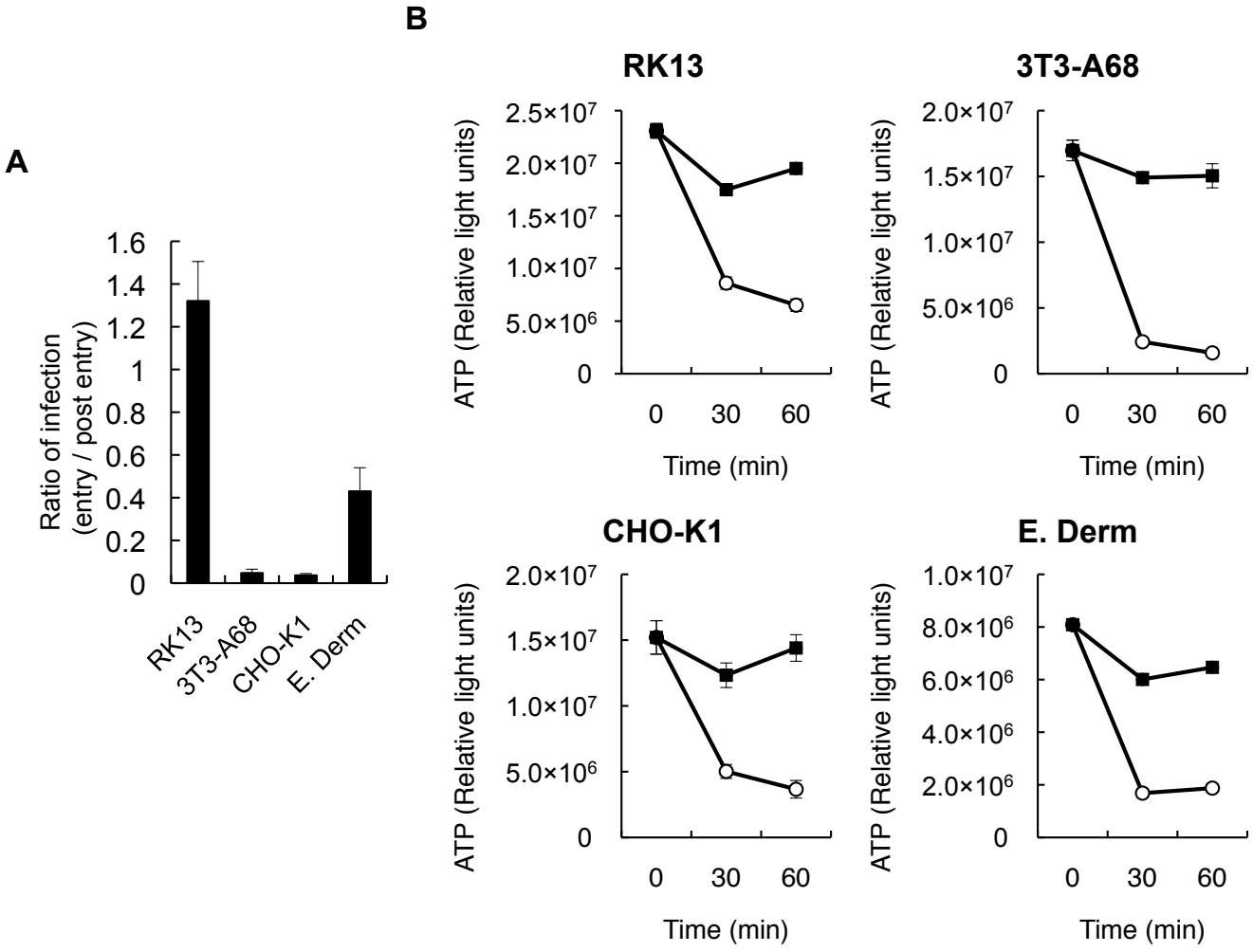

Figure 3. Effect of ATP depletion on EHV-1 entry into cells
(**A**) Effect of cellular ATP depletion on EHV-1 entry into cells. RK13, 3T3-A68, CHO-K1 and E. Derm cells were treated with ATP depletion media during or post viral entry. These cells were infected with Ab4-GFP, and GFP-positive cells were counted by flow cytometry. The number of infected cells treated with ATP depletion media post viral entry was defined as one. The graphs show the mean and standard deviation of three independent experiments. (**B**) Cellular ATP levels of each cell line with or without the ATP depletion treatment. Cells were incubated with ATP depletion media (open circles) or DMEM control media (solid squares) for the indicated time periods. Cellular ATP was measured with the CellTiter-Glo luminescent cell viability assay. Error bars represent standard deviations.

product was detected in the samples without transcriptase, amplified products were not derived from the viral genomic DNA (data not shown). I also investigated whether 3T3-A68 cells could support EHV-1 replication by evaluating the kinetics of viral growth. The extracellular titers of 3T3-A68 and E. Derm cells gradually increased with time (Fig. 4B). Conversely, EHV-1–inoculated NIH3T3 cells yielded no infectious progeny at 24 h p.i. (Fig. 4B). These results suggest that equine MHC class I molecules mediate EHV-1 entry and subsequent replication in 3T3-A68 cells.

Involvement of EHV-1 gD on equine MHC class I-mediated viral entry

Glycoprotein D (gD) of EHV-1 is known to be important for EHV-1 entry into RK13 (Whalley *et al.* 2007) and CHO-K1 cells (Van de Walle *et al.* 2008). To evaluate the role of gD in equine MHC class I-mediated entry, I tested the ability of anti-gD polyclonal antibody to block EHV-1 infection of 3T3-A68 cells. Anti-gD polyclonal antibody inhibited EHV-1 entry in a dose-dependent manner (Fig. 5A). I next generated a soluble gD-Ig fusion protein consisting of the extracellular domain of EHV-1 gD and the Fc segment of the human IgG1 and tested its ability to block EHV-1 infection of 3T3-A68 cells as previously described by Satoh *et al.* (2008). gD-Ig also inhibited EHV-1 entry into 3T3-A68 cells in a dose-dependent manner, with concentrations higher than 30 ug/ml being effective at blocking infection (Fig. 5B). Anti-gD antibody and gD-Ig also inhibited EHV-1 entry into 3T3-B118 cells, a NIH3T3-derived cell line stably expressing the other allele of equine MHC class I (data not shown). These results suggest that EHV-1 gD is involved in equine MHC class I-mediated EHV-1 entry.

To investigate the putative interaction between equine MHC class I and EHV-1 gD, lysates of cells expressing HA-tagged A68 (A68-HA) were incubated with gD-Ig fusion protein coupled magnetic beads. A68 was precipitated by gD-Ig but not by the

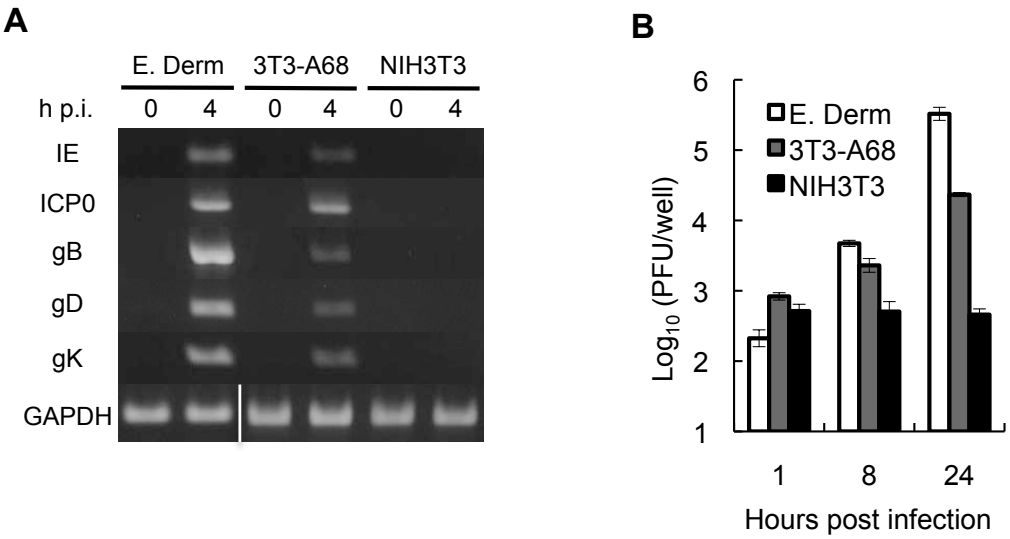

Figure 4. Effect of equine MHC class I expression on NIH3T3 cells
(**A**) Expression of viral RNAs in 3T3-A68, NIH3T3 and E. Derm cells. Cells were infected with EHV-1 Ab4-GFP, and total RNA was extracted at 0 and 4 h p.i. Immediate early (IE), early (ICP0) and late (gB, gD, gK) transcripts were detected by RT-PCR. GAPDH was used as an internal control. (**B**) Time course of viral growth in E. Derm (white bars), 3T3-A68 (gray bars) and NIH3T3 (black bars) cells. Cells were infected to Ab4-GFP at an MOI of 5 for 1h and washed with PBS to remove uninfected virus. The viral titer of each supernatant was determined by a plaque formation assay on RK13 cells. Each bar represents the amount of cell-free virus as the mean of three independent samples. Error bars show standard deviations.

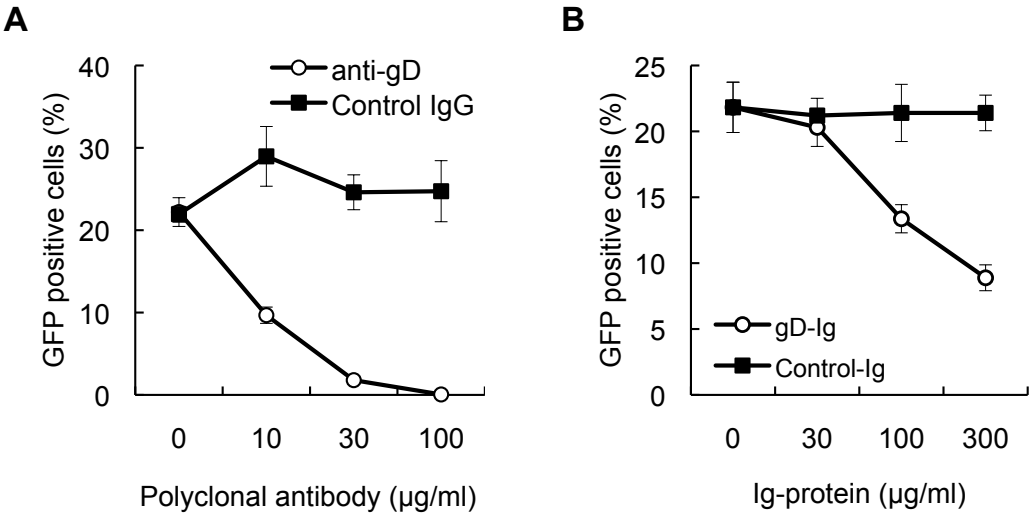

Figure 5. Involvement of EHV-1 gD in equine MHC class I-mediated viral entry
(**A**) Inhibition of EHV-1 entry by anti-gD polyclonal antibody. EHV-1 Ab4-GFP at a final MOI of 5 was incubated with anti-gD polyclonal antibody (open circles) or control rabbit IgG (solid squares) for 30 min and the virus-antibody mixture was added to 3T3-A68 cells. After incubation for 2 h, extracellular virus was inactivated by treatment with citrate buffer. GFP-positive cells were counted by flow cytometry. (**B**) Inhibition of EHV-1 entry by gD-Ig fusion protein. 3T3-A68 cells were incubated with gD-Ig (open circles) or control-Ig (solid squares) for 30 min and infected with the EHV-1 Ab4-GFP at an MOI of 5. After incubation for 2 h, extracellular virus was inactivated by treatment with citrate buffer. GFP-positive cells were counted by flow cytometry. Error bars represent standard deviations of three independent samples.

control-Ig (Fig. 6A). I also confirmed that EHV-1 gD was precipitated by the soluble A68-Ig fusion protein (Fig. 6B). Next, I analyzed the direct binding of gD to A68 expressed on the cell surface, which induced binding of gD-Ig, but not control-Ig, to the cells (Fig. 6C). Similarly, A68-Ig reacted with EHV-1 gD expressed on the cell surface (Fig. 6D). Cell surface expression of A68 and EHV-1 gD was confirmed by staining with specific antibodies (Figs. 6C and D). These results indicate that EHV-1 gD acts as a ligand for equine MHC class I molecules on the cell surface.

Anti-MHC class I antibodies block EHV-1 entry into equine cells

I investigated the involvement of MHC class I molecules in EHV-1 entry into other equine cell types that are susceptible to EHV-1 infection, such as E. Derm cells and equine PBMC. Expression of MHC class I on E. Derm cells and PBMC was confirmed by flow cytometry using the same anti-MHC class I antibodies used in Fig. 2 (Fig. 7A). After preincubation with these antibodies or the IgG isotype controls, cells were exposed to Ab4-GFP. PT85A and H58A treatment significantly inhibited virus entry into E. Derm cells (inhibition of 58% and 30% as compared to the mock treatment, respectively) (Fig. 7B). PT85A and H58A also prevented EHV-1 entry into PBMC (infection inhibition of 33% and 65%, respectively) (Fig. 7C). On the other hand, treatment with B5C did not lead to inhibition of EHV-1 entry into these cells. These results suggest that equine MHC class I molecules are involved in EHV-1 entry into different types of equine cells.

MHC class I molecules play a pivotal role in EHV-1 entry into E. Derm cells

Since PT85A markedly prevented EHV-1 entry into E. Derm cells (Fig. 7B), I postulated that EHV-1 enters equine cells mainly via a MHC class I-dependent pathway.

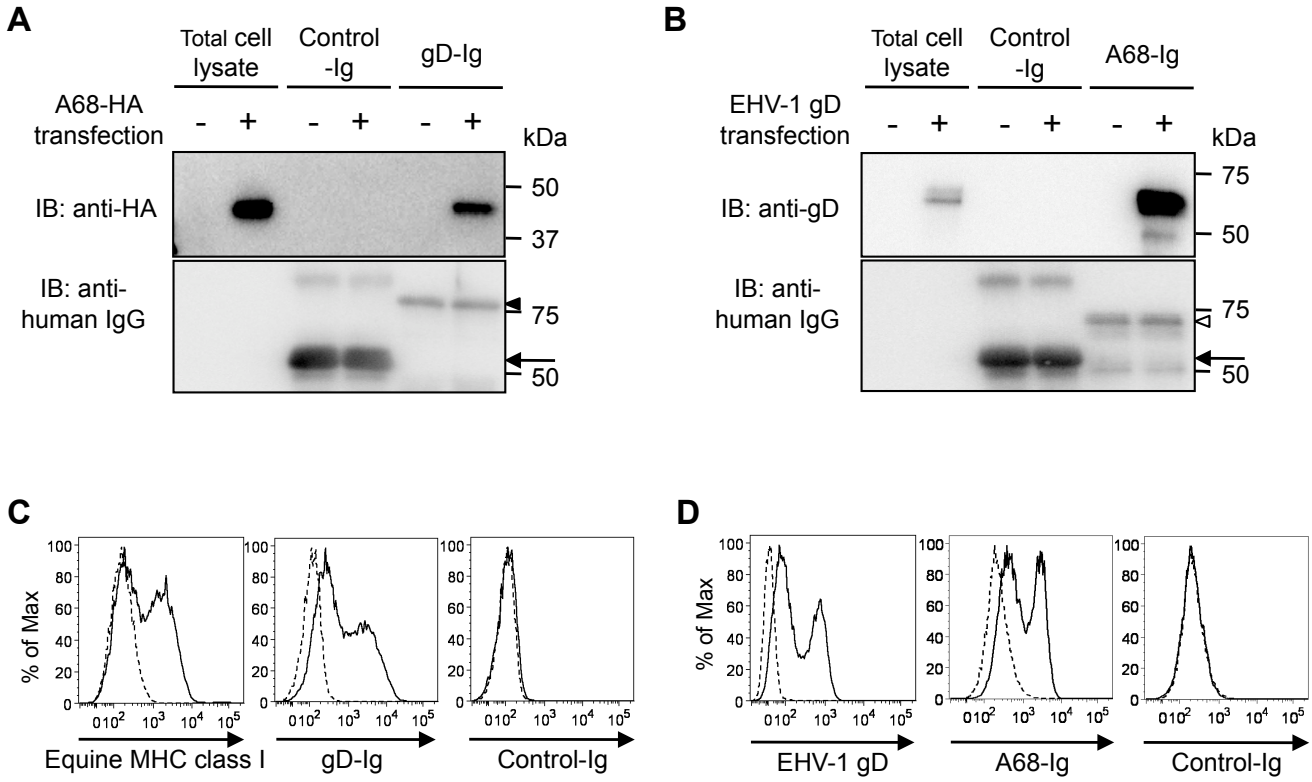

Figure 6. Interaction of equine MHC class I with EHV-1 gD
(**A** and **B**) Immunoprecipitation assay. (**A**) Protein A beads coupled with gD-Ig or control-Ig were incubated with a lysate of 293T cells co-transfected with HA-tagged A68 and equine β2m expression plasmids. (**B**) Protein A beads coupled with A68-Ig or control-Ig were incubated with a lysate of 293T cells transfected with the EHV-1 gD expression plasmid. Precipitated proteins were separated by SDS-PAGE and subjected to immunoblotting (IB) using the antibodies indicated. Solid arrowhead, open arrowhead and arrow indicate gD-Ig, A68-Ig and control Ig, respectively. (**C** and **D**) Binding assay of gD and A68. (**C**) A68 and equine β2m co-transfected 293T cells (solid line) or mock vector transfected 293T cells (dashed lines) were incubated with anti-equine MHC class I monoclonal antibody (left), gD-Ig (middle) or control-Ig (right). (**D**) 293T cells transfected with EHV-1 gD (dashed lines) or mock vector (dashed lines) were incubated with anti-gD polyclonal antibody (left), A68-Ig (middle) or control-Ig (right). Bound Ig fusion proteins were stained with PE-conjugated anti-human IgG and analyzed by flow cytometry.

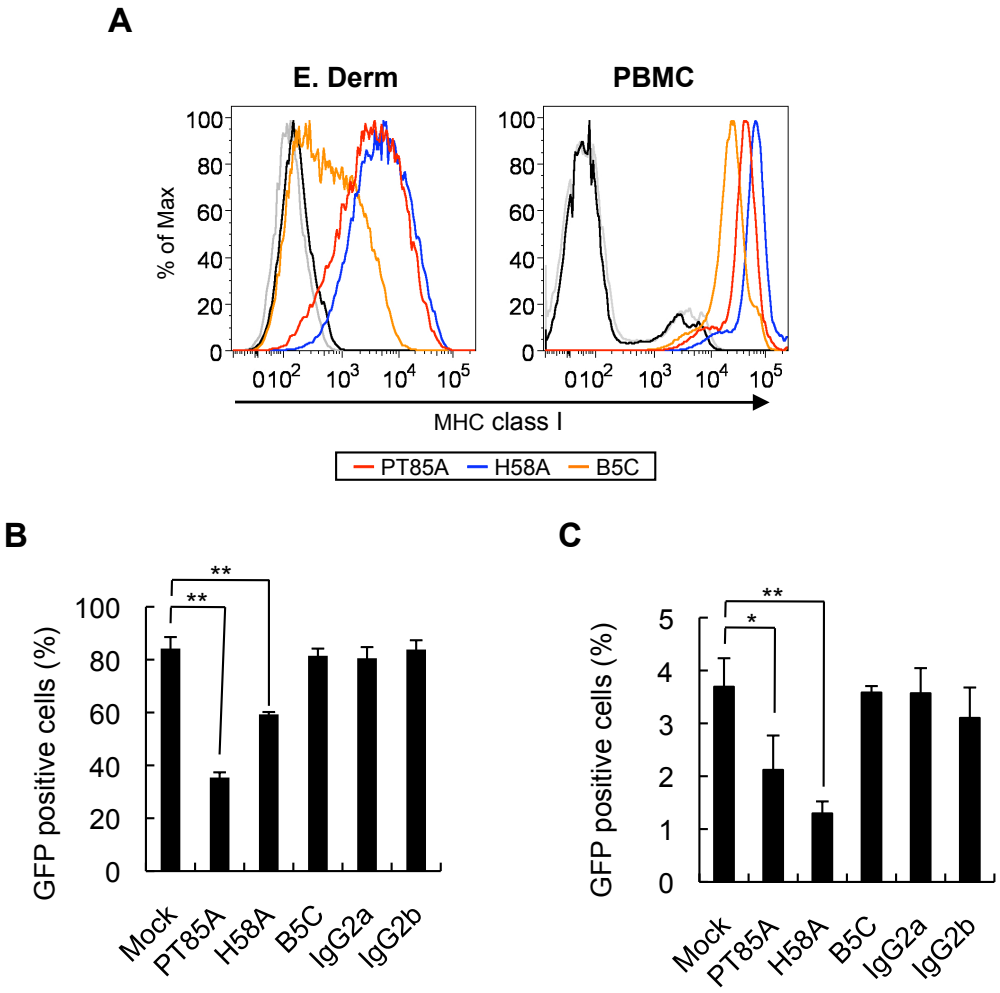

Figure 7. Inhibition of EHV-1 entry into equine cells with an anti-MHC class I antibody

(**A**) Flow cytometric detection of MHC class I expression on E. Derm and equine PBMC stained with anti-MHC class I antibody PT85A (red), H58A (blue), B5C (orange), or isotype controls IgG2a and IgG2b (black and gray, respectively).

(**B**) E. Derm and (**C**) PBMC were preincubated with 50 μg/ml of anti-MHC class I or control antibodies for 30 min, and then infected with EHV-1 Ab4-GFP at an MOI of 5 in the presence of the antibody for 2 h at 37°C. After removing virus-antibody mixtures, cells were treated with a low-pH citrate buffer to inactivate extracellular virions. Incubation was continued for a further 12 h. GFP-positive cells were counted by flow cytometry. Bars represent the means from three samples and error bars show standard deviations. Statistical significance was determined by Student's *t*-tests and is indicated by asterisks (*p < 0.05, **p < 0.01).

To test this hypothesis, I examined the effect of endogenous MHC class I gene knockdown on EHV-1 infection of E. Derm cells using lentiviral delivery of shRNA. The recombinant lentivirus would drive shRNA synthesis under the control of the H1 promoter and express mRFP1 under the control of the cytomegalovirus promoter, thereby enabling us to identify lentivirus infected cells by mRFP1 gene expression (Fig. 8G and K). A transduction efficiency higher than 95% was estimated from mRFP1 expression.

I constructed recombinant viruses carrying shRNA that targeted equine MHC class I heavy chain mRNA. However, MHC class I expression was not sufficiently reduced (data not shown), probably due to MHC class I gene polymorphisms (Figueiredo *et al.* 2006).

MHC class I molecules are composed of a single membrane-spanning heavy chain paired with a soluble protein β2m. The cell surface expression of MHC class I depends on the noncovalent binding of the heavy chain and β2m (Bjorkman & Parham 1990). Figueiredo *et al.* (2006) found that β2m-specific shRNA silenced MHC class I molecules on the cell surface. Therefore, I designed two shRNA constructs targeting equine β2m (designated as shβ2m1 and shβ2m2). Flow cytometric analysis indicated that E. Derm cells transduced with β2m-specific shRNAs showed silenced β2m expression and reduced MHC class I cell surface expression compared to non-treated cells or cells transduced with luciferase-specific shRNA (shluc) (Fig. 8A).

Non-treated or shRNA-transduced E. Derm cells were then infected with Ab4-GFP. Although there were a few GFP positive cells, almost all of the β2m-specific shRNA-transduced E. Derm cells showed neither CPE (Figs. 8F and G), nor GFP expression (Fig. 8H). In contrast, non-treated (Figs. 8B-E) and shluc-transduced (Figs. 8J-M) cells demonstrated both CPE and GFP expression after EHV-1 infection,

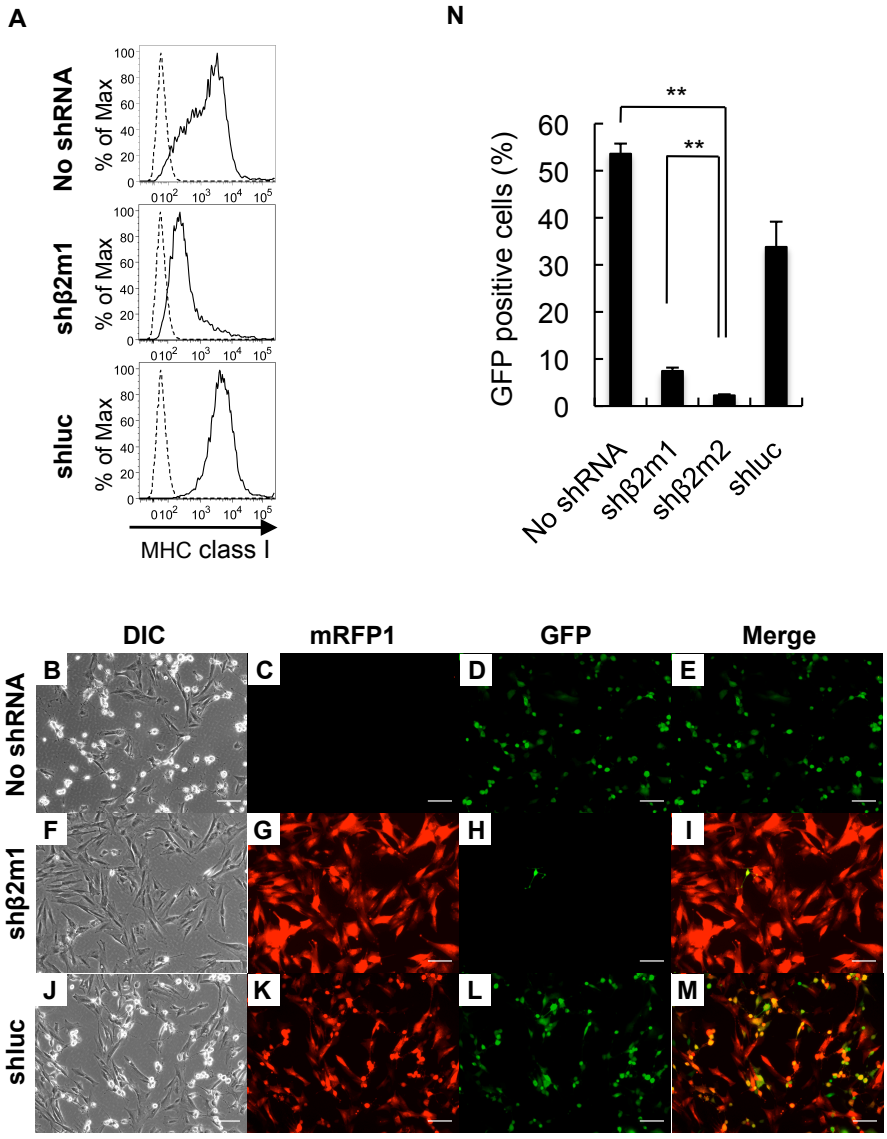

Figure 8. Knock-down of the cell surface expression of MHC class I
E. Derm cells were infected with recombinant lentiviruses carrying both shRNA and mRFP1 expression cassettes. E. Derm cells were transduced with equine β2m-specific shRNA (shβ2m1 and shβ2m2) or luciferase-specific shRNA (shluc). (**A**) Flow cytometric analysis of the cell surface expression of MHC class I. Cells transduced with shRNAs (solid lines) or non-treated E. Derm cells (dashed line) were stained with anti-MHC class I antibody PT85A. (**B-M**) Effect of shRNA transduction on the susceptibility of E. Derm cells to EHV-1. Cells were infected with Ab4-GFP at an MOI of 1 for 24 h. Transduction of shRNA lentiviral vectors was confirmed by mRFP1 expression and infection of Ab4-GFP was confirmed by GFP expression under a fluorescence microscope. Scale bars: 100 µm. (**N**) After infection with Ab4-GFP, GFP-positive cells were counted by flow cytometry. The bars represent the means from three samples and error bars show standard deviations. Statistical significance was analyzed by Student's *t*-test and is indicated by an asterisk (**p < 0.01).

indicating that these cells were still susceptible to EHV-1 infection. The number of EHV-1 infected cells was reduced in shβ2m1- and shβ2m2-transduced E. Derm cells when compared to mock cells (Fig. 8N). These results suggest that MHC class I is a major determinant of susceptibility to EHV-1 infection in E. Derm cells.

MHC class I expression on CHO-K1 cells has no role in EHV-1 infection

EHV-1 is able to infect CHO-K1 cells, which are naturally resistant to HSV-1, HSV-2, PRV and VZV entry. Therefore, I investigated whether MHC class I is also involved in EHV-1 entry into CHO-K1 cells. Anti-MHC class I antibody H58A and B5C reacted with MHC class I on CHO-K1 (Fig. 9A); however, these antibodies failed to block EHV-1 entry (Fig. 9B). PT85A did not recognize Chinese hamster's MHC class I (Fig. 9A). I also confirmed the influence of β2m knockdown on CHO-K1 cells. The surface expression of MHC class I was strongly reduced by the transduction of shRNAs targeting Chinese hamster's β2m (Fig. 9C). The levels of EHV-1 infection in β2m-knockdown cells were comparable to those in non-treated and shluc-transduced cells (Fig. 9D). These data indicate that EHV-1 does not depend on MHC class I for entry into CHO-K1 cells.

Discussion

In this study, the surface expression of equine MHC class I heavy chains cloned from EBMECs or E. Derm cells rendered mouse NIH3T3 cells susceptible to EHV-1 infection, with EHV-1 entry and subsequent replication in these cells depending on the expression of MHC class I. Pretreatment of equine cells, including primary cultured EBMECs and PBMC which are important targets of EHV-1 in vivo, with an anti-equine MHC class I monoclonal antibody inhibited EHV-1 entry. Moreover, the susceptibility

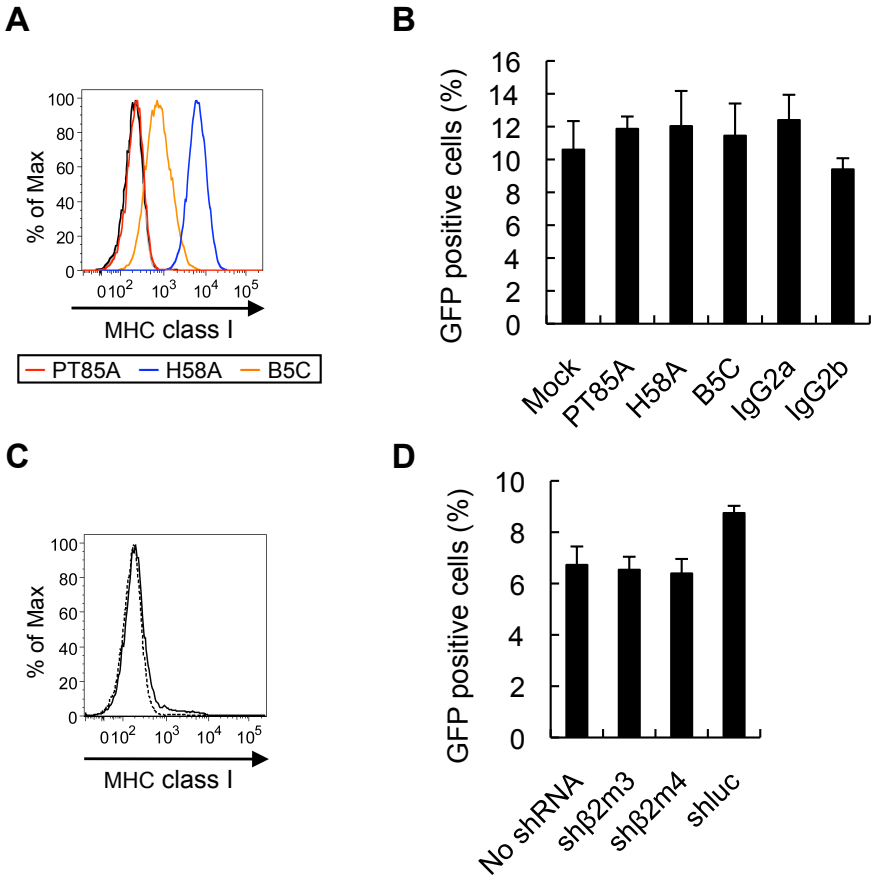

Figure 9. MHC class I-independent infection of CHO-K1 cells by EHV-1
(**A**) Flow cytometric detection of hamster MHC class I expression on CHO-K1 cells stained with anti-MHC class I antibody PT85A (red), H58A (blue), B5C (orange), or isotype controls IgG2a and IgG2b (black and gray, respectively). (**B**) CHO-K1 cells were preincubated with 50 μg/ml of anti-MHC class I or control antibodies for 30 min and then infected with the EHV-1 Ab4-GFP at an MOI of 5 in the presence of antibody for 2 h at 37°C. After removing virus-antibody mixtures, cells were treated with a low-pH citrate buffer to inactivate extracellular virions. Incubation was continued for a further 12 h. GFP-positive cells were counted by flow cytometry. Bars represent means from three samples and error bars show standard deviations. (**C** and **D**) Knock-down of the cell surface expression of MHC class I by transduction of Chinese hamster's β2m-specific shRNA (shβ2m3 and shβ2m4). (**C**) Flow cytometric analysis of the cell surface expression of MHC class I. Cells expressing shβ2m4 (solid line) and no shRNA (dashed line) were stained with anti-MHC class I antibody H58A. (**D**) Cells expressing shRNA were infected with the EHV-1 Ab4-GFP at an MOI of 1 for 24 h. GFP-positive cells were counted by flow cytometry. Bars represent means from three samples and error bars show standard deviations.

of E. Derm cells to EHV-1 infection was markedly inhibited by β2m gene knockdown, which subsequently reduced the surface expression of all MHC class I molecules. These results suggest that equine MHC class I plays an important role in EHV-1 entry into equine cells.

A mechanism of entry for EHV-1 was recently reported by another group (Kurtz *et al.* 2010); however, they demonstrated the involvement of MHC class I only in the case of EHV-1 entry into a mouse melanoma cell line with exogenously overexpressed MHC class I. Therefore, this study is the first to show that equine MHC class I molecules actually mediate EHV-1 entry into equine cell types, which are naturally susceptible to EHV-1 infection.

Alphaherpesvirus entry into target cells occurs a cascade of direct interactions between viral glycoproteins and receptors (Spear 2004; Heldwein & Krummenacher 2008). Receptors for HSV-1 on the host cell surface bind to HSV-1 gD, triggering viral entry into cells (Whitbeck *et al.* 1997; Krummenacher *et al.* 1998; Shukla *et al.* 1999). Blocking the interaction between entry receptors and gD inhibits HSV-1 entry and infection (Whitbeck *et al.* 1997; Geraghty *et al.* 1998; Shukla *et al.* 1999). A previous study showing the involvement of MHC class I in EHV-1 entry did not identify the viral protein that acts as a ligand for MHC class I (Kurtz *et al.* 2010). In this study, I demonstrated that EHV-1 gD interacts with equine MHC class I, and that viral entry into 3T3-A68 cells was inhibited by the treatment with anti-gD antibody and a soluble form of gD. These results suggest that equine MHC class I acts as an entry receptor for EHV-1 by binding to EHV-1 gD.

The data obtained in this study showed that only a fraction of NIH3T3 cells expressing MHC class I was infected with EHV-1. This finding suggests that the cell surface expression of MHC class I is not the sole determinant for the susceptibility of

NIH3T3 cells to EHV-1. Cellular factors other than equine MHC class I might be required for establishment of highly-efficient infection of NIH3T3 cells with EHV-1.

In this study, anti-MHC class I antibodies showed variable inhibition effects on EHV-1 infection in different cell types (Figs. 2 and 7). One possible explanation for this variability is that the extent of inhibition of EHV-1 entry by anti-MHC class I antibodies may be influenced by the number and/or diversity of MHC class I molecules expressed on each cell type. Since MHC molecules are polymorphic, the degrees of reactivity of monoclonal antibodies may vary among MHC class I molecules encoded by different loci.

Equine MHC class I genes are located on chromosome 20 (Ansari *et al.* 1988; Gustafson *et al.* 2003). It is still unclear how many class I genes exist within the horse genome, but the presence of up to 33 MHC class I genes and/or pseudo genes is indicated by restriction fragment length polymorphisms of the equine genome (Alexander *et al.* 1987). Moreover, 15 MHC class I loci were identified and sequenced from bacterial artificial chromosome clones containing homozygous MHC horse genes, and seven of these loci were transcribed into the mRNA in adult lymphocytes by RT-PCR (Tallmadge *et al.* 2005). Although this study showed that at least two equine MHC class I heavy chains, A68 and B118, confer susceptibility to EHV-1 infection, further studies are needed to determine whether all equine MHC class I molecules are involved in EHV-1 entry.

Although this study demonstrates the role of equine MHC class I in EHV-1 entry into equine cells, the distribution of MHC class I itself may not correlate directly with EHV-1 tissue tropism, since virtually all cell types can express MHC class I molecules (David-Watine *et al.* 1990). Therefore, host factors other than MHC class I may be involved in the observed EHV-1 tropism.

Recently, αV integrins were shown to be important for EHV-1 entry into CHO-K1 cells but not endothelial cells collected from the carotid arteries of horses, suggesting the existence of different pathways of EHV-1 entry in these cells (Van de Walle *et al.* 2008). Here, I demonstrated that MHC class I participates in EHV-1 entry into equine cells; however, pretreatment with anti-MHC class I antibody and the reduction of cell surface MHC class I expression by β2m knockdown did not alter the susceptibility of CHO-K1 cells to EHV-1. These data indicate that EHV-1 relies on different pathways for entry into different types of host cells.

The mouse intranasal infection model has many similarities to natural infection in horses. Intranasal infection of adult mice causes local viral replication in the respiratory mucosa, with formation of intranuclear inclusions and subsequent rhinopneumonitis (Awan *et al.* 1990; Inazu *et al.* 1993; Bartels *et al.* 1998). However, this model does not develop encephalomyelitis, a characteristic of viral infection in CNS endothelial cells. The results obtained in this study suggest that EHV-1 is unlikely to utilize mouse MHC class I as a factor for entry into mouse cells because the NIH3T3 cells used in this study (which are not susceptible to EHV-1 infection) expressed mouse MHC class I molecules (haplotype $H2^q$) on their surface (Seliger *et al.* 1998; Herrmann *et al.* 2004). Interestingly, in contrast to the EBMECs that express equine MHC class I and were thus susceptible to EHV-1 infection, mouse brain microvascular endothelial cells are completely resistant to EHV-1 infection and are not susceptible to viral entry (Hasebe *et al.* 2006). Therefore, the differences between the host factors underlying EHV-1 entry in equine and mouse cells may contribute to the difference in EHV-1 pathogenicity between the horse and the mouse model.

In summary, I demonstrated that equine MHC class I molecule acts as a functional gD receptor for EHV-1 entry and infection, which contributes to the understanding of

the molecular mechanisms of EHV-1 entry into cells (summarized in Table 2). In recent years, outbreaks of the neurological form of EHV-1 have occurred at various equine facilities worldwide. An effective approach to therapy and prevention is still under investigation. Transgenic mice expressing equine MHC class I on their endothelial cells, already under development, might provide a suitable model for the study of EHV-1 pathogenesis, aiding in the investigation of novel vaccines and drugs for EHV-1 infection.

Table 2 Cellular entry pathways of EHV-1

Cell types	Species	Entry pathways	Receptor molecules	References
Equine aortic endothelial cells	Horse	Direct fusion	Unclear	Van de Walle et al. (2009)
Equine brain microvascular endothelial cells	Horse	Endocytosis	MHC class I	Hasebe et al. (2006), Hasebe et al. (2009), Current study
Equine peripheral blood mononuclear cells	Horse	Endocytosis	MHC class I and Integrin	Van de Walle et al. (2009), Current study
E. Derm cells	Horse	Direct fusion and Endocytosis	MHC class I	Frampton et al. (2007), Hasebe et al. (2009), Current study
CHO-K1 cells	Hamster	Endocytosis	Integrin	Frampton et al. (2007), Van de Walle et al. (2009)
RK13 cells	Rabbit	Direct fusion	Unclear	Frampton et al. (2007)

Summary

The endotheliotropism of EHV-1 leads to encephalomyelitis secondary to vasculitis and thrombosis in the infected horse CNS. To identify the host factors involved in EHV-1 infection of CNS endothelial cells, I performed functional cloning using an EBMEC cDNA library. Exogenous expression of equine MHC class I heavy chain genes conferred susceptibility to EHV-1 infection in mouse NIH3T3 cells, which are not naturally susceptible to EHV-1 infection. Equine MHC class I molecules bound to EHV-1 gD, and both anti-gD antibodies and a soluble form of gD blocked viral entry into NIH3T3 cells stably expressing the equine MHC class I heavy chain (3T3-A68 cells). Treatment with an anti-equine MHC class I monoclonal antibody blocked EHV-1 entry into 3T3-A68 cells, E. Derm cells and EBMECs. In addition, inhibition of cell surface expression of MHC class I molecules in E. Derm cells drastically reduced their susceptibility to EHV-1 infection. These results suggest that equine MHC class I is a functional gD receptor that plays a pivotal role in EHV-1 entry into equine cells.

Chapter 2

Distribution of MHC class I mRNA in equine tissues

Introduction

In the previous chapter, I identified equine MHC class I as an entry receptor of EHV-1. Little is known, however, about the correlation of MHC class I distribution with the cellular tropism of EHV-1. Although MHC class I is known to be distributed broadly in mammalian bodies, neurons do not express detectable MHC class I levels under normal conditions in the CNS of human and rats (Lampson & Hickey 1986; David-Watine *et al.* 1990; Vass & Lassmann 1990; Höftberger *et al.* 2004). Importantly, histopathological studies of EHV-1 encephalomyelitis reported that neurons are far less susceptible to EHV-1 infection than endothelial cells (Patel *et al.* 1982; Edington *et al.* 1986). In this chapter, I investigated the expression of equine MHC class I genes in various equine tissue. In adult horse brain tissue, *in situ* hybridization revealed localized expression of MHC class I in endothelial cells. I next confirmed that primary cultured equine neurons are resistant to EHV-1 infection. This study provides new insights into the mechanism of EHV-1 endotheliotropism and a potential way to treat and prevent this infectious disease.

Materials and Methods

Preparation of an RNA probe

A cDNA fragment corresponding to equine MHC class I A68 was subcloned by PCR using primers 5’-GGC GAA TTC CTA CCT GGA GGG CAC GTG CG-3’ and 5’-ACT CAA GCT TTG GTC TCC ACA AGC TCT GTG-3’. The PCR products were

digested with restriction enzymes *EcoRI* and *HindIII*, and then cloned into the pGEM-3Z vector (Promega). Strand-specific RNA probes were prepared using a digoxigenin (DIG)-based RNA-labeling kit (SP6/T7; Roche Diagnostics, Indianapolis, IN). To obtain templates for RNA transcription, plasmid DNA containing the cloned cDNA was linearized with *EcoRI* to synthesize the antisense RNA, or with *HindIII* to synthesize the sense RNA, in the presence of DIG-11-UTP. The labeled probes generated from 1 μg of plasmid DNA were precipitated with ethanol, dissolved in 50 μl of RNase-free water (Invitrogen), and stored at -80°C.

Northern hybridization

Total RNA was extracted from the tissues of 1-year-old female horse with the TRIzol reagent (Invitrogen). RNA samples (5 μg) were electrophoresed through a 1.2% agarose-2.2 M formaldehyde gel and stained with ethidium bromide to verify equal RNA loading in all lanes. The RNAs were transferred to a Hybond-N^+ nylon membrane (GE Healthcare), fixed to the membrane with a UV cross-linker (UVP, Upland, CA), and then baked at 80°C for 30 min.

Hybridization was performed by the method of Shifman and Stein (1995) with minor modifications. Briefly, membranes were prehybridized in 0.25 M Na_2HPO_4 (pH 7.2), 10% SDS, 1 mM ethylenediaminetetraaceticacid (EDTA), and 2% blocking reagent (Roche Diagnostics) at 68°C for 3 h. Hybridization was performed in the same buffer containing the DIG-labeled RNA probe for A68 (100 ng/ml) at 68°C for 16 h. After hybridization, membranes were washed three times for 20 min each in 25 mM Na_2HPO_4 (pH 7.2), 1% SDS, and 1 mM EDTA at 68°C. Hybridization complexes were visualized with alkaline phosphatase-conjugated anti-DIG antibody (Roche Diagnostics) and disodium 3-(4-methoxyspiro{1,2-dioxetane-3,2'-(5'-chloro)tricyclo

[3.3.1.1^{3,7}]decan}-4-yl) phenyl phosphate (CSPD) (Tropix, Bedford, MA), and observed with an LAS-1000 (GE Healthcare).

In situ hybridization

In situ hybridization was performed as described previously (Kimura *et al.* 2004). Briefly, 4-μm sections of paraffin-embedded tissues were mounted on Matsunami Adhesive Silane (MAS)-coated glass slides (Matsunami Glass, Osaka, Japan). The slides were dewaxed in xylene, washed with ethanol, and air-dried, digested with 300 μg/ml proteinase K (Invitrogen) for 30 min at 37°C, fixed in 4% paraformaldehyde (PFA) for 10 min, and then washed with 0.1 M phosphate buffer (PB; pH 7.4). Slides were treated with 0.2 N HCl for 10 min, washed with PB, acetylated for 10 min in 0.1 M triethanolamine (pH 8.0) containing 0.25% acetic anhydride, washed, dehydrated in an ascending ethanol series, and air-dried.

DIG-labeled RNA probes for A68 were diluted 1:100 in hybridization solution (50% formamide, 10 mM Tris–HCl, pH 7.6, 200 μg/ml tRNA, 1×Denhardt's solution, 10% dextran sulphate, 600 mM NaCl, 1 mM EDTA, and 0.25% SDS), denatured at 85°C for 3 min, and dropped onto the sections. Sections were heated at 95°C for 5 min, put on ice for 1 min, and hybridized for 16 h in a moist chamber at 47°C. Subsequent stringent washing was performed at the same temperature. After removing the coverslips into 5× SSC (0.75 M NaCl, 75 mM sodium citrate), the slides were washed once for 30 min with 2× SSC containing 50% formamide and twice for 20 min with 0.2× SSC. Hybridization probes were detected with anti-DIG antibodies coupled to alkaline phosphatase and developed according to the manufacturer's instructions (DIG Nucleic Acid Detection Kit; Roche Diagnostics). Hybridization with DIG-labeled sense probes was used as a negative control. All sections were counterstained in methyl green

solution (WAKO, Osaka, Japan).

Cells and viruses

Neurons were prepared from adult horse dorsal root ganglia (DRG) by the method of Sango *et al*. (2007), and maintained in Neurobasal A supplemented with B27 supplement, 5 ng/ml mouse nerve growth factor and 10 μg/ml gentamicin (all from Invitrogen). Cells were maintained at 37°C in 5% CO_2. The EHV-1 mutant Ab4-GFP, which contains a GFP expression cassette between ORF 62 and ORF 63 (Ibrahim *et al.* 2004), was generously provided by Dr. Fukushi (Gifu University, Gifu, Japan). Stock viruses were grown in E. Derm cells. The viral titer was determined by plaque formation on RK13 cells.

Indirect immunofluorescence staining

Cells on a 35-mm glass-base dish (Asahi Techno Glass, Tokyo, Japan) were infected with EHV-1 Ab4-GFP at an MOI of 100 for 12 h. After washing with PBS, cells were fixed with 4% paraformaldehyde and permeabilized with 0.1% Triton X-100 in PBS. Blocking was performed with PBS containing 5% BSA at room temperature. Cells were stained with an anti-tubulin β3 (Millipore) and Alexa Fluor 594 goat anti-mouse IgG antibody (Invitrogen). Signals were observed under an inverted fluorescence microscope (Olympus).

Results

Distribution of equine MHC class I heavy chain mRNA

To evaluate the equine MHC class I heavy chain mRNA expression in horse tissues, I performed Northern hybridization using an A68-specific DIG-labeled RNA probe.

Northern hybridization with an antisense probe demonstrated that MHC class I heavy chain mRNAs (1.8 kilobase) were detectable in all tissues examined, with relatively high expression levels in the lung, spleen, and kidney (Fig. 10). No signal was observed by hybridization with a sense probe (data not shown).

In situ localization of equine MHC class I heavy chain mRNA in adult horse brain

I next performed *in situ* hybridization using the same probe to investigate the MHC class I heavy chain mRNA distribution in adult horse cerebral cortex tissues. *In situ* hybridization revealed the expression of MHC class I heavy chain mRNA in the capillary endothelial cells (Fig. 11A), but not in the neurons or glial cells (Fig. 11B), in the brain. Specific hybridization signals were not detected using a sense probe (Fig. 11C).

Horse neurons are resistant to EHV-1 infection

To determine the susceptibility of horse neurons to EHV-1 infection, I prepared neurons from adult horse DRG. Indirect immunofluorescence staining showed that the culture contains both tubulin β3-positive neurons and tubulin β3-negative non-neuronal cells (Fig. 12). Cells were infected with EHV-1 Ab4-GFP strain at an MOI of 100. Neurons, stained for tubulin β3, showed no GFP signal, despite that a lot of tubulin β3-negative non-neuronal cells were infected with EHV-1 (Fig. 12).

Discussion

I detected MHC class I heavy chain mRNA in various tissues in the adult horse by Northern hybridization. Virtually all cell types can express MHC class I molecules (David-Watine *et al.* 1990), suggesting that the distribution itself may not correlate

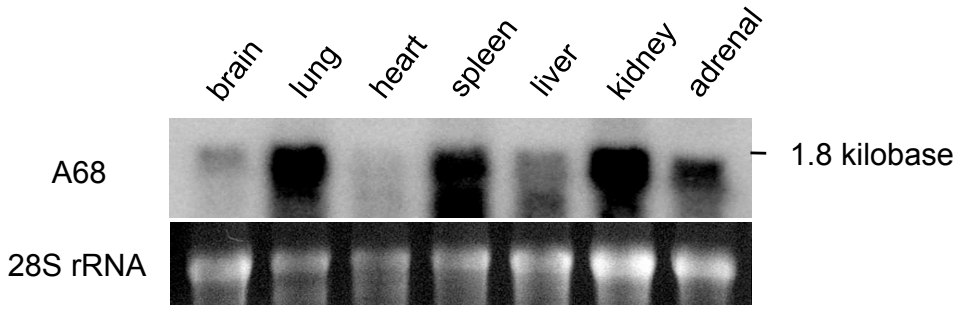

Figure 10. Distribution of equine MHC class I heavy chain mRNA in horse tissues
Northern blot hybridization of equine MHC class I heavy chain mRNA in various horse tissues. Five micrograms of total RNA were loaded per lane. Ethidium bromide fluorescence of 28S ribosomal RNA was used as an RNA-loading control.

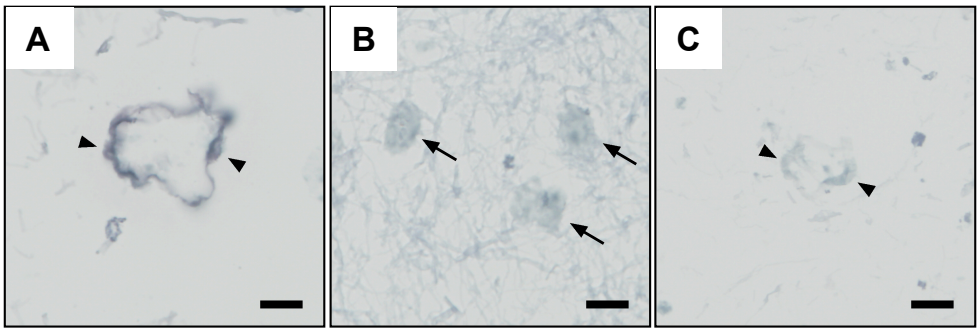

Figure 11. *In situ* hybridization of equine MHC class I heavy chain mRNA in horse brain tissue

In situ hybridization with an antisense (**A** and **B**) or sense (**C**) RNA probe specific for A68 in the horse brain tissue. Arrowheads show endothelial cells (**A** and **C**) and arrows show neurons (**B**). Nuclei were counter stained with methyl green. Scale bars: 20 μm.

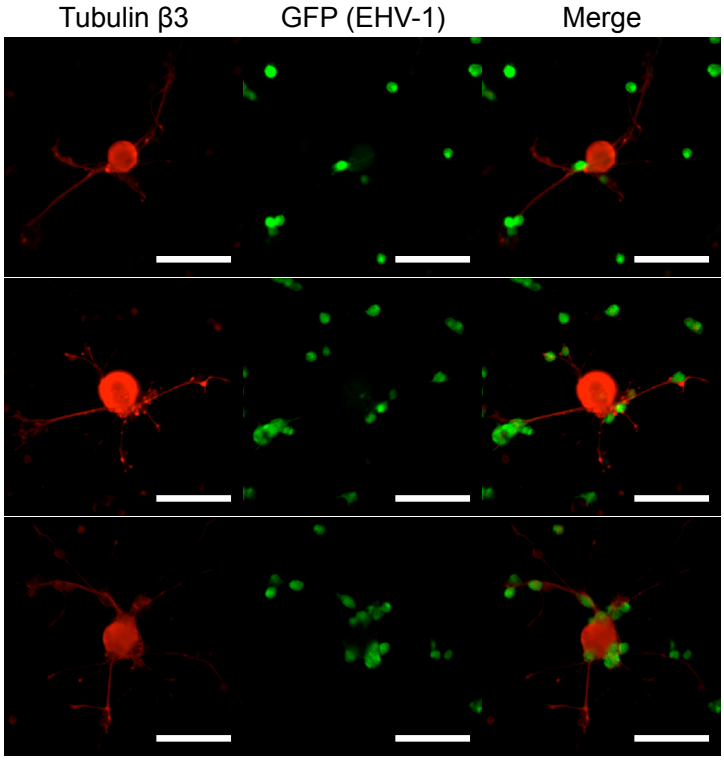

Figure 12. Immunofluorescence analysis of primary cultured horse neurons after EHV-1 infection

Dissociated cell culture of adult horse DRG were infected with the EHV-1 Ab4-GFP strain at an MOI of 100 for 12 h. Neurons were immunostained using tubulin β3 antibody followed by Alexa 594-conjugated goat anti-mouse IgG antibody. Scale bars: 100 μm.

with EHV-1 tissue tropism. However, *in situ* hybridization data showed that MHC class I mRNA is limited to endothelial cells within adult horse brains. Constitutive MHC class I expression in the rodent and human CNS also occurs mainly in endothelial cells, whereas neurons and glial cells do not express detectable MHC class I levels under normal conditions (Lampson & Hickey 1986; Vass & Lassmann 1990; Höftberger *et al.* 2004). Interestingly, unlike other alphaherpesvirus encephalitises in which the viruses replicate in neurons and glial cells [i.e., Herpes simplex virus type 1 (HSV-1) in humans and Pseudorabies virus (PRV) in pigs], EHV-1 preferentially infects endothelial cells but generally does not infect the neurons or glial cells (Edington *et al.* 1986; Whitwell & Blunden 1992). The endothelial localization of MHC class I mRNA may be related to the susceptibility of endothelial cells to EHV-1 in the CNS.

In this study, I confirmed that primary cultured horse neurons were unsusceptible to EHV-1 infection. Although this finding was consistent with the paucity of neuronal infection in EHV-1 encephalomyelitis, the relationship between the levels of MHC class I and EHV-1 susceptibility should be determined in future.

In conclusion, this study shows the endothelial localization of MHC class I in normal horse brain tissue. In contrast to primary cultured EBMECs as shown in chapter 1, primary equine neurons were resistant to EHV-1 infection. These results suggest that the localized expression of MHC class I may make endothelial cells a principal initial target in EHV-1 encephalomyelitis development.

Summary

The endotheliotropism of EHV-1 leads to encephalomyelitis secondary to vasculitis and thrombosis in the infected horse CNS. Unlike other alphaherpesviruses, EHV-1 does not generally infect neurons in the natural host. However, little is known about the host factors that determine the susceptibility of CNS endothelial cells to EHV-1 infection. I previously identified equine MHC class I as a molecule participate in EHV-1 entry into horse cells. Equine MHC class I heavy chain mRNA was detected in various equine tissues by Northern hybridization. However, *in situ* hybridization revealed equine MHC class I heavy chain mRNA expression in the endothelial cells of small blood vessels, but not in the neurons or glial cells, in the adult horse brain. Neurons isolated from adult horse DRG are resistant to EHV-1 infection. These results suggest that the endothelial localization of MHC class I expression in the CNS may be involved in EHV-1 encephalomyelitis development.

General Conclusion

EHV-1 is known to cause respiratory disease, abortion, and encephalomyelitis in horses. After airborne transmission, EHV-1 infects respiratory epithelial cells and mononuclear leukocytes in the local lymph nodes, resulting in leukocyte-associated viremia. The virus then infects blood vessel endothelial cells in the CNS. The inflammation following endothelial viral replication triggers encephalomyelitis secondary to vasculitis, thrombosis, and ischemic damage of the CNS. The mechanism of how EHV-1 exhibits this endotheliotropism remains to be elucidated.

In chapter 1, I performed functional cloning using an equine brain microvascular endothelial cell cDNA library and identified that equine MHC class I heavy chain conferred susceptibility to EHV-1 infection in mouse NIH3T3 cells, which are naturally resistant to EHV-1 infection. Anti-equine MHC class I monoclonal antibody, anti-EHV-1 gD polyclonal antibody, and a soluble gD-Ig fusion protein inhibited EHV-1 infection of NIH3T3 cells stably expressing the equine MHC class I heavy chain gene. The gD-Ig fusion protein bound specifically to equine MHC class I. These data demonstrate that equine MHC class I acts as an entry receptor for EHV-1 by binding to EHV-1 gD.

I next investigated the involvement of MHC class I molecules in EHV-1 entry into equine cell types that are naturally susceptible to EHV-1 infection. Anti-equine MHC class I monoclonal antibody blocked EHV-1 entry into E. Derm cells, primary EBMECs and primary equine PBMC. The susceptibility of E. Derm cells to EHV-1 infection was drastically reduced by β2m gene knockdown, which subsequently reduced the surface expression of all MHC class I molecules. These results indicate that equine MHC class I molecules are involved in EHV-1 entry into different types of equine cells.

EHV-1 efficiently enters and replicates in CHO-K1 cells lacking known

alphaherpesvirus receptors. Therefore, I examined the role of hamster MHC class I in EHV-1 entry into CHO-K1 cells. Pretreatment with anti-MHC class I monoclonal antibody and the reduction of cell surface MHC class I expression by β2m knockdown did not alter the susceptibility of CHO-K1 cells to EHV-1, suggesting the presence of MHC class I-independent pathway for EHV-1 entry into CHO-K1 cells.

In chapter 2, I investigated the localization of equine MHC class I gene expression in a horse tissue. Northern hybridization analysis for detection of MHC class I gene expression in the major organs of the adult horse demonstrated that MHC class I heavy chain mRNAs were detectable in all tissues examined. *In situ* hybridization revealed equine MHC class I heavy chain mRNA expression in the endothelial cells of small blood vessels, but not in the neurons or glial cells, in the adult horse brain. This result suggests that the localized expression of equine MHC class I on CNS endothelial cells may be related to the susceptibility of endothelial cells to EHV-1 in the CNS.

The entry of virus into target cells is a crucial step in the establishment of infection. In this thesis, I demonstrated that equine MHC class I is a bona fide receptor of EHV-1 entry into equine cells. This finding contributes to the understanding of molecular mechanism of EHV-1 entry into cells. Antibodies and recombinant proteins used in this study inhibited EHV-1 entry and infection, suggesting that blocking the interaction between MHC class I and EHV-1 gD is a possible candidate of protection against EHV-1–induced diseases.

References

Alexander, A., Bailey, E. & Woodward, J. (1987) Analysis of the equine lymphocyte antigen system by Southern blot hybridization. *Immunogenetics* **25**, 47-54.

Ansari, H., Hediger, R., Fries, R. & Stranzinger, G. (1988) Chromosomal localization of the major histocompatibility complex of the horse (ELA) by in situ hybridization. *Immunogenetics* **28**, 362-364.

Arii, J., Goto, H., Suenaga, T., Oyama, M., Kozuka-Hata, H., Imai, T., Minowa, A., Akashi, H., Arase, H., Kawaoka, Y. & Kawaguchi, Y. (2010) Non-muscle myosin IIA is a functional entry receptor for herpes simplex virus-1. *Nature* **467**, 859-862.

Awan, A., Chong, Y. & Field, H. (1990) The pathogenesis of equine herpesvirus type 1 in the mouse: a new model for studying host responses to the infection. *J Gen Virol* **71**, 1131-1140.

Bartels, T., Steinbach, F., Hahn, G., Ludwig, H. & Borchers, K. (1998) In situ study on the pathogenesis and immune reaction of equine herpesvirus type 1 (EHV-1) infections in mice. *Immunology* **93**, 329-334.

Bjorkman, P. & Parham, P. (1990) Structure, function, and diversity of class I major histocompatibility complex molecules. *Annu Rev Biochem* **59**, 253-288.

David-Watine, B., Israël, A. & Kourilsky, P. (1990) The regulation and expression of MHC class I genes. *Immunol Today* **11**, 286-292.

Edington, N., Bridges, C. & Patel, J. (1986) Endothelial cell infection and thrombosis in paralysis caused by equid herpesvirus-1: equine stroke. *Arch Virol* **90**, 111-124.

Figueiredo, C., Seltsam, A. & Blasczyk, R. (2006) Class-, gene-, and group-specific HLA silencing by lentiviral shRNA delivery. *J Mol Med* **84**, 425-437.

Frampton, A.J., Goins, W., Cohen, J., von Einem, J., Osterrieder, N., O'Callaghan, D. & Glorioso, J. (2005) Equine herpesvirus 1 utilizes a novel herpesvirus entry receptor. *J Virol* **79**, 3169-3173.

Frampton, A.J., Stolz, D., Uchida, H., Goins, W., Cohen, J. & Glorioso, J. (2007) Equine herpesvirus 1 enters cells by two different pathways, and infection requires the activation of the cellular kinase ROCK1. *J Virol* **81**, 10879-10889.

Geraghty, R., Krummenacher, C., Cohen, G., Eisenberg, R. & Spear, P. (1998) Entry of alphaherpesviruses mediated by poliovirus receptor-related protein 1 and poliovirus receptor. *Science* **280**, 1618-1620.

Gustafson, A., Tallmadge, R., Ramlachan, N., Miller, D., Bird, H., Antczak, D., Raudsepp, T., Chowdhary, B. & Skow, L. (2003) An ordered BAC contig map of the equine major histocompatibility complex. *Cytogenet Genome Res* **102**, 189-195.

Hasebe, R., Kimura, T., Nakamura, K., Ochiai, K., Okazaki, K., Wada, R. & Umemura, T. (2006) Differential susceptibility of equine and mouse brain microvascular

endothelial cells to equine herpesvirus 1 infection. *Arch Virol* **151**, 775-786.

Hasebe, R., Sasaki, M., Sawa, H., Wada, R., Umemura, T. & Kimura, T. (2009) Infectious entry of equine herpesvirus-1 into host cells through different endocytic pathways. *Virology* **393**, 198-209.

Heerkens, T. (2009) Equine herpesvirus-1, non-neurogenic pathotype, in a 9-year-old American Saddlebred with neurological signs. *Can Vet J* **50**, 297-300.

Heldwein, E. & Krummenacher, C. (2008) Entry of herpesviruses into mammalian cells. *Cell Mol Life Sci* **65**, 1653-1668.

Herrmann, F., Lehr, H., Drexler, I., Sutter, G., Hengstler, J., Wollscheid, U. & Seliger, B. (2004) HER-2/neu-mediated regulation of components of the MHC class I antigen-processing pathway. *Cancer Res* **64**, 215-220.

Holmes, E. & Ellis, S. (1999) Evolutionary history of MHC class I genes in the mammalian order Perissodactyla. *J Mol Evol* **49**, 316-324.

Höftberger, R., Aboul-Enein, F., Brueck, W., Lucchinetti, C., Rodriguez, M., Schmidbauer, M., Jellinger, K. & Lassmann, H. (2004) Expression of major histocompatibility complex class I molecules on the different cell types in multiple sclerosis lesions. *Brain Pathol* **14**, 43-50.

Ibrahim, e.S., Pagmajav, O., Yamaguchi, T., Matsumura, T. & Fukushi, H. (2004)

Growth and virulence alterations of equine herpesvirus 1 by insertion of a green fluorescent protein gene in the intergenic region between ORFs 62 and 63. *Microbiol Immunol* **48**, 831-842.

Inazu, M., Tsuha, O., Kirisawa, R., Kawakami, Y. & Iwai, H. (1993) Equid herpesvirus 1 infection in mice. *J Vet Med Sci* **55**, 119-121.

Katayama, K., Wada, K., Miyoshi, H., Ohashi, K., Tachibana, M., Furuki, R., Mizuguchi, H., Hayakawa, T., Nakajima, A., Kadowaki, T., Tsutsumi, Y., Nakagawa, S., Kamisaki, Y. & Mayumi, T. (2004) RNA interfering approach for clarifying the PPARgamma pathway using lentiviral vector expressing short hairpin RNA. *FEBS Lett* **560**, 178-182.

Kimura, T., Hasebe, R., Mukaiya, R., Ochiai, K., Wada, R. & Umemura, T. (2004) Decreased expression of equine herpesvirus-1 early and late genes in the placenta of naturally aborted equine fetuses. *J Comp Pathol* **130**, 41-47.

Kohn, C.W., Reed, S.M., Sofaly, C.D., Henninger, R.W., Saville, W.J., Allen, G.P. & Premanadan, C. (2006) Transmission of EHV-1 by Horses with EHV-1 Myeloencephalopathy: Implications for Biosecurity and Review. *Clinical Techniques in Equine Practice* **5**, 60-66.

Krummenacher, C., Nicola, A., Whitbeck, J., Lou, H., Hou, W., Lambris, J., Geraghty, R., Spear, P., Cohen, G. & Eisenberg, R. (1998) Herpes simplex virus glycoprotein D can bind to poliovirus receptor-related protein 1 or herpesvirus entry mediator, two

structurally unrelated mediators of virus entry. *J Virol* **72**, 7064-7074.

Kurtz, B.M., Singletary, L.B., Kelly, S.D. & Frampton, A.R. (2010) Equus caballus major histocompatibility complex class I is an entry receptor for equine herpesvirus type 1. *J Virol* **84**, 9027-9034.

Lampson, L. & Hickey, W. (1986) Monoclonal antibody analysis of MHC expression in human brain biopsies: tissue ranging from "histologically normal" to that showing different levels of glial tumor involvement. *J Immunol* **136**, 4054-4062.

Li, Q., Ali, M. & Cohen, J. (2006) Insulin degrading enzyme is a cellular receptor mediating varicella-zoster virus infection and cell-to-cell spread. *Cell* **127**, 305-316.

Miyoshi, H., Blömer, U., Takahashi, M., Gage, F. & Verma, I. (1998) Development of a self-inactivating lentivirus vector. *J Virol* **72**, 8150-8157.

Montgomery, R., Warner, M., Lum, B. & Spear, P. (1996) Herpes simplex virus-1 entry into cells mediated by a novel member of the TNF/NGF receptor family. *Cell* **87**, 427-436.

Nicola, A., McEvoy, A. & Straus, S. (2003) Roles for endocytosis and low pH in herpes simplex virus entry into HeLa and Chinese hamster ovary cells. *J Virol* **77**, 5324-5332.

Osterrieder, N. (1999) Construction and characterization of an equine herpesvirus 1 glycoprotein C negative mutant. *Virus Res* **59**, 165-177.

Osterrieder, N. & Van de Walle, G.R. (2010) Pathogenic potential of equine alphaherpesviruses: the importance of the mononuclear cell compartment in disease outcome. *Vet Microbiol* **143**, 21-28.

Patel, J., Edington, N. & Mumford, J. (1982) Variation in cellular tropism between isolates of equine herpesvirus-1 in foals. *Arch Virol* **74**, 41-51.

Sango, K., Yanagisawa, H. & Takaku, S. (2007) Expression and histochemical localization of ciliary neurotrophic factor in cultured adult rat dorsal root ganglion neurons. *Histochem Cell Biol* **128**, 35-43.

Satoh, T., Arii, J., Suenaga, T., Wang, J., Kogure, A., Uehori, J., Arase, N., Shiratori, I., Tanaka, S., Kawaguchi, Y., Spear, P., Lanier, L. & Arase, H. (2008) PILRalpha is a herpes simplex virus-1 entry coreceptor that associates with glycoprotein B. *Cell* **132**, 935-944.

Seliger, B., Harders, C., Lohmann, S., Momburg, F., Urlinger, S., Tampé, R. & Huber, C. (1998) Down-regulation of the MHC class I antigen-processing machinery after oncogenic transformation of murine fibroblasts. *Eur J Immunol* **28**, 122-133.

Shifman, M. & Stein, D. (1995) A reliable and sensitive method for non-radioactive northern blot analysis of nerve growth factor mRNA from brain tissues. *J Neurosci Methods* **59**, 205-208.

Shukla, D., Liu, J., Blaiklock, P., Shworak, N., Bai, X., Esko, J., Cohen, G., Eisenberg, R., Rosenberg, R. & Spear, P. (1999) A novel role for 3-O-sulfated heparan sulfate in herpes simplex virus 1 entry. *Cell* **99**, 13-22.

Spear, P. (2004) Herpes simplex virus: receptors and ligands for cell entry. *Cell Microbiol* **6**, 401-410.

Stierstorfer, B., Eichhorn, W., Schmahl, W., Brandmüller, C., Kaaden, O. & Neubauer, A. (2002) Equine herpesvirus type 1 (EHV-1) myeloencephalopathy: a case report. *J Vet Med B Infect Dis Vet Public Health* **49**, 37-41.

Studdert, M., Hartley, C., Dynon, K., Sandy, J., Slocombe, R., Charles, J., Milne, M., Clarke, A. & El-Hage, C. (2003) Outbreak of equine herpesvirus type 1 myeloencephalitis: new insights from virus identification by PCR and the application of an EHV-1-specific antibody detection ELISA. *Vet Rec* **153**, 417-423.

Suenaga, T., Satoh, T., Somboonthum, P., Kawaguchi, Y., Mori, Y. & Arase, H. (2010) Myelin-associated glycoprotein mediates membrane fusion and entry of neurotropic herpesviruses. *Proc Natl Acad Sci U S A* **107**, 866-871.

Tallmadge, R., Lear, T. & Antczak, D. (2005) Genomic characterization of MHC class I genes of the horse. *Immunogenetics* **57**, 763-774.

Ui-Tei, K., Naito, Y., Takahashi, F., Haraguchi, T., Ohki-Hamazaki, H., Juni, A., Ueda, R. & Saigo, K. (2004) Guidelines for the selection of highly effective siRNA sequences

for mammalian and chick RNA interference. *Nucleic Acids Res* **32**, 936-948.

Van de Walle, G., Peters, S., VanderVen, B., O'Callaghan, D. & Osterrieder, N. (2008) Equine herpesvirus 1 entry via endocytosis is facilitated by alphaV integrins and an RSD motif in glycoprotein D. *J Virol* **82**, 11859-11868.

Vass, K. & Lassmann, H. (1990) Intrathecal application of interferon gamma. Progressive appearance of MHC antigens within the rat nervous system. *Am J Pathol* **137**, 789-800.

Warner, M., Geraghty, R., Martinez, W., Montgomery, R., Whitbeck, J., Xu, R., Eisenberg, R., Cohen, G. & Spear, P. (1998) A cell surface protein with herpesvirus entry activity (HveB) confers susceptibility to infection by mutants of herpes simplex virus type 1, herpes simplex virus type 2, and pseudorabies virus. *Virology* **246**, 179-189.

Whalley, J., Ruitenberg, K., Sullivan, K., Seshadri, L., Hansen, K., Birch, D., Gilkerson, J. & Wellington, J. (2007) Host cell tropism of equine herpesviruses: glycoprotein D of EHV-1 enables EHV-4 to infect a non-permissive cell line. *Arch Virol* **152**, 717-725.

Whitbeck, J., Peng, C., Lou, H. *et al.* (1997) Glycoprotein D of herpes simplex virus (HSV) binds directly to HVEM, a member of the tumor necrosis factor receptor superfamily and a mediator of HSV entry. *J Virol* **71**, 6083-6093.

Whitwell, K. & Blunden, A. (1992) Pathological findings in horses dying during an

outbreak of the paralytic form of Equid herpesvirus type 1 (EHV-1) infection. *Equine Vet J* **24**, 13-19.

Acknowledgement

I would like to acknowledge Professor Hirofumi Sawa, Department of Molecular Pathobiology, Research Center for Zoonosis Control, Hokkaido University, for his valuable advices and detained review of this manuscript.

Great appreciation is extended to Professor Takashi Umemura, Laboratory of Comparative Pathology, Department of Veterinary Clinical Sciences, Graduate School of Veterinary Medicine, Hokkaido University, Professor Kazuhiko Ohashi, Laboratory of Infectious diseases, Department of Disease Control, Graduate School of Veterinary Medicine, Hokkaido University, and Professor Ayato Takada, Department of Global Epidemiology, Research Center for Zoonosis Control, Hokkaido University for reviewing the manuscript, valuable advices and suggestions.

I am also deeply grateful to Associate Professor Takashi Kimura Department of Molecular Pathobiology, Research Center for Zoonosis Control, Hokkaido University and Lecturer Rie Hasebe, Department of Applied Veterinary Sciences, Laboratory of Veterinary Hygiene, Graduate School of Veterinary Medicine, Hokkaido University for valuable advices, suggestions and encouragement throughout this study.

I would like to acknowledge Dr. Hideto Fukushi, Laboratory of Veterinary Microbiology, Faculty of Applied Biological Sciences, Gifu University, for providing EHV-1 mutant strain Ab4-GFP; Dr. Hisashi Arase, Department of Immunochemistry, Research Institute for Microbial Diseases, Osaka University, for providing pME18S Ig fusion protein expression vector; Dr. Hiroyuki Miyoshi, Subteam for Manipulation of Cell Fate, RIKEN Bioresource Center, for providing lentiviral vector system; Dr. Hiroyuki Taniyama, Department of Veterinary Pathology, School of Veterinary Medicine, Rakuno Gakuen University, for providing horse tissues; Dr. Rikio Kirisawa, Department of Veterinary Microbiology, School of Veterinary Medicine, Rakuno

Gakuen University, for providing rabbit polyclonal antibody to EHV-1.

Finally, thanks are also due to all members of the Department of Molecular Pathobiology, Research Center for Zoonosis Control, Hokkaido University.

Summary in Japanese

ウマヘルペスウイルス1型 (EHV-1) はヘルペスウイルス科アルファヘルペスウイルス亜科に属し、馬に脳脊髄炎、流産、鼻肺炎を惹き起こす。罹患馬に重篤な神経症状をもたらす脳脊髄炎では、中枢神経系の血管内皮細胞へのウイルス感染が病態形成に大きな役割を果たすことが明らかになっている。しかしながら、EHV-1 の血管内皮向性を規定する宿主因子に関しては不明な点が多い。

第 1 章では、ウマ脳微小血管内皮細胞（EBMECs）より作製した cDNA 発現ライブラリーを用いて、EHV-1 レセプターのクローニングを試みた。スクリーニングの結果、EHV-1 非感受性細胞であるマウス由来細胞株 NIH3T3 に EHV-1 感受性を付与する遺伝子として、ウマ主要組織適合遺伝子複合体（MHC）class I 重鎖遺伝子を同定した。ウマ MHC class I 重鎖遺伝子を安定発現させた NIH3T3 細胞への EHV-1 感染は、抗 MHC class I モノクローナル抗体、抗 EHV-1 glycoprotein D (gD) ポリクローナル抗体および gD ヒトイムノグロブリン（Ig）融合タンパク（gD-Ig）によって阻害された。また、gD-Ig はウマ MHC class I 分子に特異的に結合した。これらの結果から、ウマ MHC class I が EHV-1 gD をリガンドとするエントリーレセプターであることが明らかになった。

次に、EHV-1 の自然宿主である馬の細胞を用いて、EHV-1 感染におけるウマ MHC class I 分子の関与を解析した。ウマ真皮由来株化細胞 E. Derm、EBMECs、ウマ末梢血単核球（PBMC）を抗 MHC class I モノクローナル抗体で前処理すると、EHV-1 感染は阻害された。また、β2 ミクログロブリン（β2m）分子の発現のノックダウンによって MHC class I 分子の細胞表面発現を抑制した E. Derm 細胞は、EHV-1 感受性が顕著に減少した。以上の結果から、ウマ MHC class I は EHV-1 のウマ細胞内侵入に重要な役割を果たすことが明らかになった。

EHV-1 は既知のアルファヘルペスウイルスレセプターを発現していないハムスター由来細胞株 CHO-K1 に感染し増殖する。そこで、EHV-1 の CHO-K1 細胞

への侵入にハムスターMHC class I 分子が関与しているかどうかを検討した。抗 MHC class I モノクローナル抗体の前処理によって EHV-1 感染は阻害されなかった。また、β2m 分子の発現のノックダウンによって CHO-K1 細胞表面における MHC class I 分子の発現を抑制しても、EHV-1 感受性の変化は認められなかった。従って、CHO-K1 細胞には MHC class I に依存しない EHV-1 の細胞内侵入機構が存在することが示唆された。

第 2 章では、ウマ組織における MHC class I 遺伝子発現の局在を解析した。成馬の全身主要臓器をノーザンハイブリダイゼーションにより解析した結果、検索した全臓器においてウマ MHC class I mRNA が検出された。また、成馬脳組織に対して *in situ* ハイブリダイゼーション法を施行したところ、ウマ MHC class I mRNA の局在を示すシグナルは血管内皮細胞に限局しており、神経細胞を含むその他の細胞にシグナルは認められなかった。以上の結果より、馬の中枢神経系における MHC class I の遺伝子発現は EHV-1 の標的細胞である血管内皮細胞に限局しており、MHC class I の遺伝子発現が EHV-1 の脳脊髄炎の病態形成に関与している可能性が示唆された。

ウイルスの細胞内侵入は、感染の成立に重要なステップである。本研究によって、ウマ MHC class I が EHV-1 のエントリーレセプターとして機能することが明らかとなり、これは EHV-1 の細胞内侵入機構の解明において重要な知見であると考えられる。また、抗体や組換えタンパクを用いた感染実験の結果より、EHV-1 gD と MHC class I の結合阻害が、EHV-1 感染症の治療法として有用である可能性が示唆された。